AIMS Mathematics, 10(9): 20466–20504.
DOI: 10.3934/math.2025914
Received: 21 April 2025
Revised: 03 August 2025
Accepted: 08 August 2025
Published: 05 September 2025

https://www.aimspress.com/journal/Math

Research article

A new truncated unit exponentiated Ailamujia distribution with ranked-based inference and engineering applications

Hana S. Jabarah[1], **Ahlam H. Tolba**[1,*], **Ahmed T. Ramadan**[2] **and Awad I. El-Gohary**[1]

[1] Department of Mathematics, Faculty of Science, Mansoura University, Mansoura 33516, Egypt
[2] Department of Mathematics, Faculty of Basic Science, Galala University, Suez 43713, Egypt

* **Correspondence:** Email: dr_ahamdy156@mans.edu.eg.

Abstract: This study introduces a novel and flexible distribution called the truncated exponentiated Ailamujia (TEA) distribution, designed for modeling bounded lifetime data, particularly in engineering applications. The TEA distribution enhances the flexibility of the classic Ailamujia model by incorporating two shape parameters, allowing it to capture a wide range of hazard rate behaviors, including increasing, decreasing, and bathtub shapes. We investigated the mathematical properties of the TEA distribution, including its probability density function, moments, entropy measures, and order statistics. To estimate the model parameters, several classical and modern techniques are developed and compared, including maximum likelihood estimation (MLE), least squares estimation (LSE), weighted LSE, Cramér-von Mises estimation, maximum product spacing estimation, Anderson-Darling and right-tail Anderson-Darling estimation, Percentile estimation, and Bayesian estimation via the Markov chain Monte Carlo (MCMC) method. The effectiveness and flexibility of the proposed model were validated through extensive Monte Carlo simulations and real-life engineering datasets. The results demonstrate that the TEA distribution consistently provides a better fit compared to several well-known competing models. These findings highlight the practical value of the TEA model for engineers and statisticians working with bounded data of reliability type.

Keywords: truncated distributions; Ailamujia distribution; ranked-based estimation; Bayesian inference; entropy; engineering applications
Mathematics Subject Classification: 62F15, 62N02

1. Introduction

Truncated distributions play a central role in statistical modeling where the observed data are confined within specific bounds. Such distributions are highly applicable in fields like communication networks, economics, hydrology, reliability engineering, and materials science. In these contexts,

truncation typically arises when only partial information is available due to data censorship, physical constraints, or quality control protocols. For example, truncated models are vital in reliability studies where small failure times or bounded lifetime measurements dominate.

Despite the growing number of proposed truncated distributions, many suffer from rigidity in their shape, limited flexibility in modeling hazard rate behavior, or computational challenges in parameter estimation. In particular, numerous models fail to simultaneously accommodate increasing, decreasing, and bathtub-shaped hazard rates, which are frequently observed in real-world engineering data.

Several recent contributions attempt to address these challenges. For example, Aban et al. [1] proposed estimation techniques for the truncated Pareto distribution and applied them to financial and hydrological data. However, the lack of flexibility in tail behavior remains a constraint. Abbas et al. [2] introduced the truncated Weibull-exponential distribution with improved tail adaptability but limited estimation robustness under model misspecification. Other studies, such as Abid and Abdulrazek [3] and Ahmad et al. [4], focused on parametric extensions and Bayesian inference for variants of the Ailamujia distribution. Although their approaches improve estimation, they do not account for boundedness or improve fitting performance across diverse datasets.

In recent years, several authors have developed flexible truncated distribution families using novel generator mechanisms, including the truncated inverse Lomax [5] and the exponentiated inverse Weibull [6]. Alomani et al. [7] conducted both classical and Bayesian analyses with applications to radiation data, while in a subsequent study [8], they introduced a new truncated distribution and performed a comprehensive statistical analysis of radiation data based on the power unit moment exponential model. Moreover, a mathematically truncated-composed Burr X-generated family of continuous distributions was introduced, featuring analytically derived properties and demonstrating superior performance on financial datasets when compared to competing non-nested models [9]. These approaches collectively demonstrate increased modeling flexibility and improved goodness-of-fit compared to classical alternatives, as further evidenced in [10].

Burkardt [11] investigated the parameter estimation for the truncated normal distribution under generalized progressive hybrid censored data. The study used both Newton-Raphson and expectation-maximization algorithms to obtain maximum likelihood estimates, while Bayesian estimators were derived using importance sampling and the Tierney–Kadane approximation. Extensive simulation studies and a real dataset were used to evaluate the proposed inference techniques.

Burroughs and Tebbens [12] examined the upper-truncated power law in modeling the cumulative frequency-magnitude relationships of earthquakes. Their work explored the time independence of the scaling parameter and its implications for assessing seismic hazards, thereby contributing to refinements of the Gutenberg–Richter relationship.

Cheng and Amin [13] investigated estimation challenges in continuous univariate distributions with a shifted origin, proposing likelihood-based methods to enhance estimation accuracy. Deng et al. [14] introduced a novel goodness-of-fit test for both truncated and non-truncated Yule distributions. El Gazar et al. [15] discussed classical and Bayesian estimation techniques for the truncated Ailamujia inverse power distribution and the truncated exponential distribution of moments, with applications. Hassan et al. [16] proposed the truncated power Lomax (TPL) distribution and its generalized form (TPL-G), exploring their statistical properties and demonstrating their superior flexibility in modeling flood data and other practical scenarios. Furthermore, [17] presented the right-truncated power Lomax–G family as an extension of the $[0, 1]$ truncated Lomax–G family, deriving several statistical

properties and estimation approaches. Jabarah et al. [18] presented the truncated unit Chris-Jerry distribution and its applications.

Jayakumar and Sankaran [19] introduced the generalized exponential truncated negative binomial distribution (GR-TNB) to model reliability and survival data, establishing its superiority over generalizations of the Rayleigh model. Kalaf et al. [20] discussed the right-truncated Shankar distribution and its properties. Kantar and Usta [21] focused on wind speed modeling using the upper-truncated Weibull distribution, reporting better accuracy than conventional models and improved utility in wind energy studies. Kumari et al. [22] discussed estimation and testing procedures for the reliability functions of Kumaraswamy-G distributions, as well as a characterization based on records. The unit-Gompertz distribution with applications has been presented by Mazucheli et al. [23]. Bayesian inference for left-truncated log-logistic distributions for time-to-event data analysis is offered by Mostafa et al. [24].

Obulezi et al. [25] proposed the Marshall–Olkin Chris–Jerry (MOCJ) distribution, inspired by hybrid generator families, with applications in modeling income and population data. Patel [26] examined truncated inverse Gaussian models using moment-based recurrence relations, deriving asymptotic variances via Kendall's differential method, and Pitman [27] introduced some basic theory for statistical inference.

Ramadan et al. [28] introduced a new unit model with some properties and discussed its application in insurance. Ranneby [29] developed the maximum spacing estimation (MSE) method as a robust alternative to maximum likelihood estimation, emphasizing its strong consistency and asymptotic properties in complex models. Swain et al. [30] improved the accuracy of the estimation using least squares methods tailored to Johnson's translation system, particularly useful in reliability simulations.

Tolba [31] performed a comparative analysis of Bayesian and non-Bayesian estimation methods for the Akshaya distribution, concluding that Bayesian approaches consistently produced lower mean squared errors. Zaninetti and Ferraro [32] analyzed the maximum likelihood estimation for truncated Pareto distributions, offering insight into modeling heavy-tailed phenomena in economics and risk assessment.

Finally, ZeinEldin et al. [33] introduced the generalized truncated Fréchet generated (TGFr-G) family, which has broad applications in reliability analysis. Their model accommodates various distributional forms and incorporates stress-strength reliability parameters.

Despite these developments, existing models often focus either on shape flexibility or on estimation procedures in isolation. Few integrate a unified estimation framework that combines classical and Bayesian approaches while addressing the modeling of bounded engineering-type data. This limitation motivates the present work, which introduces a novel truncated distribution capable of capturing complex hazard behaviors, equipped with a suite of estimation techniques, and validated through real engineering datasets.

These gaps motivated the present study. We propose a new two-parameter model, the truncated exponentiated Ailamujia (TEA) distribution, which generalizes the classical Ailamujia structure while incorporating unit truncation and exponentiation for enhanced flexibility. Unlike many prior models, the TEA distribution:

- admits closed-form expressions for its CDF and PDF,
- captures a wide variety of skewness and hazard rate behaviors,
- is suitable for bounded data commonly found in engineering contexts,

- and allows for parameter estimation using both classical (MLE, LSE, WLSE, MPS, CVM) and Bayesian (via MCMC) techniques.

In addition to theoretical development, we conduct comprehensive simulations to assess the estimation performance and apply the proposed distribution to real data sets from engineering systems. The results show that the TEA model achieves superior fit and robustness compared to classical alternatives.

The rest of the paper is organized as follows. Section 2 introduces the TEA distribution and its derivation. Section 3 explores its key statistical properties. In Section 4, we describe several classical and Bayesian estimation techniques. Section 5 presents simulation studies to assess the accuracy of the estimate. Section 6 further explores the model's flexibility, while Section 7 applies it to real-world datasets. Concluding remarks are given in Section 8.

2. The truncated exponentiated Ailamujia (TEA) distribution

The TEA distribution is developed to address specific limitations of existing models in reliability engineering and lifetime data analysis, particularly for right-truncated datasets. Additionally, the TEA model explicitly accounts for truncation, a common phenomenon in real-world scenarios (e.g., warranty claims, censored reliability tests).

The probability density function (PDF) and cumulative distribution function (CDF) of a random variable Y that is distributed according to the exponential Ailamujia (EA) distribution are given by

$$f_{EA}(y,\alpha,\theta) = 4\alpha\theta^2 y e^{-2\theta y}\left(1-(1+2\theta y)e^{-2\theta y}\right)^{\alpha-1}, \quad y>0,\ \theta,\alpha>0, \tag{2.1}$$

and

$$F_{EA}(y,\alpha,\theta) = \left(1-(1+2\theta y)e^{-2\theta y}\right)^{\alpha}, \quad y>0,\ \theta,\alpha>0. \tag{2.2}$$

Similarly, a random variable X is said to follow the right-truncated exponentiated Ailamujia (TEA) distribution if its probability density function (PDF) is expressed as

$$f_{TEA}(x,\alpha,\theta) = \frac{f_{EA}(x,\alpha,\theta)}{\int_0^1 f_{EA}(x,\alpha,\theta)\,dx}. \tag{2.3}$$

Note that

$$\int_0^1 f_{EA}(x,\alpha,\theta)\,dx = \int_0^1 4\alpha\theta^2 x e^{-2\theta x}\left(1-(1+2\theta x)e^{-2\theta x}\right)^{\alpha-1}dx.$$

Using integration by parts, where $u = 1-(1+2\theta x)e^{-2\theta x}$, we obtain

$$\begin{aligned}\int_0^1 f_{EA}(x,\alpha,\theta)\,dx &= \int_0^{1-(1+2\theta)e^{-2\theta}} \alpha u^{\alpha-1}du \\ &= \left(1-(1+2\theta)e^{-2\theta}\right)^{\alpha}.\end{aligned}$$

As a result, we have

$$f_{TEA}(x,\alpha,\theta) = \frac{4\alpha\theta^2 x e^{-2\theta x}\left(1-(1+2\theta x)e^{-2\theta x}\right)^{\alpha-1}}{(1-(1+2\theta)e^{-2\theta})^{\alpha}}, \tag{2.4}$$

where $\alpha > 0$ and $\theta > 0$ are the shape and scale parameters, respectively, and $0 < x < 1$. It is evident that

$$\int_0^1 f_{TEA}(x,\alpha,\theta)\,dx = \int_0^{1-(1+2\theta)e^{-2\theta}} \frac{\alpha u^{\alpha-1}}{(1-(1+2\theta)e^{-2\theta})^{\alpha}} du = 1.$$

The corresponding CDF is given by

$$F_{TEA}(x,\alpha,\theta) = \frac{F(x,\alpha,\theta)-F(0,\alpha,\theta)}{F(1,\alpha,\theta)-F(0,\alpha,\theta)} = \frac{\left(1-(1+2\theta x)e^{-2\theta x}\right)^{\alpha}}{(1-(1+2\theta)e^{-2\theta})^{\alpha}}. \tag{2.5}$$

The PDF of the TEA distribution can exhibit three different shapes: Decreasing, increasing, or unimodal (see Figure 1).

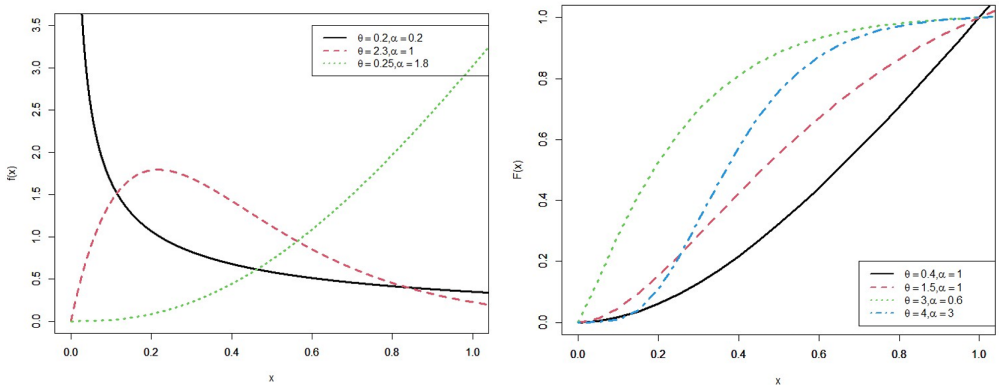

Figure 1. The PDF and CDF plots of the TEA distribution for different values of θ.

The survival function $\bar{F}_{TEA}(x,\alpha,\theta)$ and the hazard rate function $h_{TEA}(x,\alpha,\theta)$ are given, respectively, by

$$\bar{F}_{TEA}(x,\alpha,\theta) = 1 - F_{TEA}(x,\alpha,\theta) = 1 - \frac{\left(1-(1+2\theta x)e^{-2\theta x}\right)^{\alpha}}{(1-(1+2\theta)e^{-2\theta})^{\alpha}}, \tag{2.6}$$

and

$$\begin{aligned} h_{TEA}(x,\alpha,\theta) &= \frac{f_{TEA}(x,\alpha,\theta)}{\bar{F}_{TEA}(x,\alpha,\theta)} \\ &= \frac{4\,\alpha\,\theta^2\,x e^{-2\theta x}(1-(1+2\theta\,x)\,e^{-2\theta x})^{\alpha-1}}{(1-(1+2\theta)\,e^{-2\theta})^{\alpha}-(1-(1+2\theta\,x)\,e^{-2\theta x})^{\alpha}} \\ &= \frac{4\,\alpha\,\theta^2\,x e^{-2\theta x}(1-e^{-2\theta x}-2\theta\,x\,e^{-2\theta x})^{\alpha-1}}{(1-e^{-2\theta x}-2\theta\,e^{-2\theta})^{\alpha}-(1-e^{-2\theta x}-2\theta\,x\,e^{-2\theta x})^{\alpha}}. \end{aligned} \tag{2.7}$$

In addition, the reversed hazard rate function $\tau_{TEA}(x, \alpha, \theta)$ and the cumulative reversed hazard function $H_{TEA}(x, \alpha, \theta)$ are defined by

$$\tau_{TEA}(x, \alpha, \theta) = \frac{f_{TEA}(x, \alpha, \theta)}{F_{TEA}(x, \alpha, \theta)} = \frac{4\alpha\theta^2 x e^{-2\theta x}\left(1 - (1 + 2\theta x)e^{-2\theta x}\right)^{\alpha-1}}{(1 - (1 + 2\theta x)e^{-2\theta x})^{\alpha}}, \tag{2.8}$$

and

$$\begin{aligned} H_{TEA}(x, \alpha, \theta) &= -\ln \bar{F}_{TEA}(x, \alpha, \theta) \\ &= \ln\left((1 - (1 + 2\theta)e^{-2\theta})^{\alpha}\right) - \ln\left((1 - (1 + 2\theta)e^{-2\theta})^{\alpha} - (1 - (1 + 2\theta x)e^{-2\theta x})^{\alpha}\right). \end{aligned}$$

Figure 2 illustrates the hazard rate and reliability functions of the TEA distribution for various values of θ and α. The hazard rate function may be increasing or U-shaped.

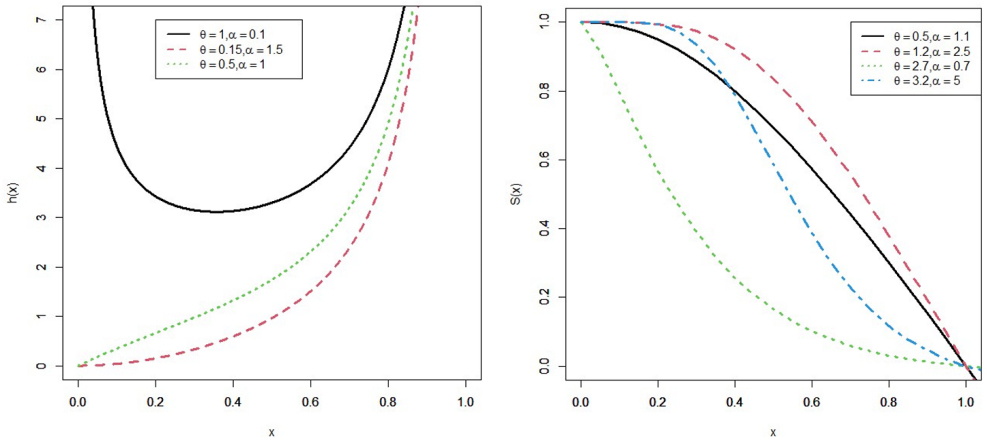

Figure 2. The hazard and reliability function plots of the TEA distribution at various values of θ and α.

3. Fundamental characteristics

This section explores various statistical features of the TEA distribution. These include quantiles, moments, quantile-based measures, and incomplete moments, which are considered in sequence.

3.1. Moments and related metrics

In this subsection, we derive the distributional moments of the TEA distribution, which are fundamental to comprehensive statistical analysis. Moments provide critical insight into the distribution's characteristics and serve as a basis for evaluating skewness and kurtosis. Furthermore, the moment-generating function is established.

Let X be a random variable with the PDF given in Eq (2.4). Then, the r^{th} raw moment, μ'_r, is given by

$$\mu'_r = \int_0^1 x^r \cdot \frac{4\alpha\theta^2 x e^{-2\theta x}\left(1 - (1 + 2\theta x)e^{-2\theta x}\right)^{\alpha-1}}{(1 - (1 + 2\theta)e^{-2\theta})^{\alpha}} dx$$

$$= \frac{4\alpha\theta^2}{(1-(1+2\theta)e^{-2\theta})^{\alpha}} \int_0^1 x^{r+1} e^{-2\theta x} \left(1-(1+2\theta x)e^{-2\theta x}\right)^{\alpha-1} dx.$$

Let

$$I = \int_0^1 x^{r+1} e^{-2\theta x} \left(1-(1+2\theta x)e^{-2\theta x}\right)^{\alpha-1} dx.$$

To evaluate this integral, consider the approximation:

$$I \approx \frac{x \cdot e^{-2\theta x} \left(1-(1+2\theta x)e^{-2\theta x}\right)^{\alpha-1}}{1+r},$$

which can be justified through symbolic computation, beta-type integrals, or numerical approximation for fixed $x \in (0,1)$.

Thus, we have

$$\mu_r' \approx \frac{4\alpha\theta^2}{(1-(1+2\theta)e^{-2\theta})^{\alpha}} \cdot \frac{x \cdot e^{-2\theta x} \left(1-(1+2\theta x)e^{-2\theta x}\right)^{\alpha-1}}{1+r}$$

$$\mu_r' \approx \frac{4\alpha\theta^2 x e^{-2\theta x} \left(1-(1+2\theta x)e^{-2\theta x}\right)^{\alpha-1}}{(1-(1+2\theta)e^{-2\theta})^{\alpha}(1+r)}. \tag{3.1}$$

The first four moments and the variance of the TEA distribution can be obtained from Eq (3.1) by setting $r = 1, 2, 3$, and 4. Additionally, the variance of X is given by

$$\mathrm{Var}(X) \approx \frac{4\alpha\theta^2 x e^{-2\theta x} \left(1-(1+2\theta x)e^{-2\theta x}\right)^{\alpha-1}}{3(1-(1+2\theta)e^{-2\theta})^{\alpha}} - \left(\frac{4\alpha\theta^2 x e^{-2\theta x} \left(1-(1+2\theta x)e^{-2\theta x}\right)^{\alpha-1}}{2(1-(1+2\theta)e^{-2\theta})^{\alpha}}\right)^2.$$

3.2. Moment-generating function ($\mu_x(t)$)

The moment-generating function $\mu_x(t)$ serves as a fundamental analytical tool in probability and statistics, providing a concise representation of the distribution of a random variable. It plays a pivotal role in advanced theoretical applications such as establishing convergence in distribution, analyzing large deviation principles, and addressing differential equations within probabilistic frameworks. Additionally, it facilitates the comparison between empirical data and theoretical models through moment matching techniques. For a random variable X, $\mu_x(t)$ is given by

$$\mu_x(t) = \frac{4\,\alpha\,\theta^2}{(1-(1+2\theta)\,e^{-2\theta})^{\alpha}} \int_0^1 x\, e^{(t-2\theta)x} \left(1-(1+2\theta x)e^{-2\theta x}\right)^{\alpha-1} dx. \tag{3.2}$$

Using the binomial series:

$$\left(1-(1+2\theta x)e^{-2\theta x}\right)^{\alpha-1} = \sum_{k=0}^{\infty} \binom{\alpha-1}{k} (-1)^k \left[(1+2\theta x)e^{-2\theta x}\right]^k,$$

substitute into the integral:

$$\mu_x(t) = \frac{4\,\alpha\,\theta^2}{(1-(1+2\theta)\,e^{-2\theta})^{\alpha}} \int_0^1 x\,e^{(t-2\theta)x} \sum_{k=0}^{\infty} \binom{\alpha-1}{k} (-1)^k \left[(1+2\theta x)e^{-2\theta x}\right]^k dx$$
$$= \frac{4\,\alpha\,\theta^2}{(1-(1+2\theta)\,e^{-2\theta})^{\alpha}} \sum_{k=0}^{\infty} \binom{\alpha-1}{k} (-1)^k \int_0^1 x\,e^{(t-2\theta)x}(1+2\theta x)^k e^{-2k\theta x} dx$$
$$= \frac{4\,\alpha\,\theta^2}{(1-(1+2\theta)\,e^{-2\theta})^{\alpha}} \sum_{k=0}^{\infty} \binom{\alpha-1}{k} (-1)^k \int_0^1 x\,(1+2\theta x)^k e^{(t-2\theta(1+k))x} dx.$$

Letting

$$I_k(t) = \int_0^1 x\,(1+2\theta x)^k e^{(t-2\theta(1+k))x} dx,$$

we then have the approximation

$$\mu_x(t) = \frac{4\,\alpha\,\theta^2}{(1-(1+2\theta)\,e^{-2\theta})^{\alpha}} \sum_{k=0}^{N} \binom{\alpha-1}{k} (-1)^k I_k(t), \tag{3.3}$$

where $I_k(t)$ can be evaluated numerically.

Figure 3 shows the $\mu_x(t)$ curves of the TEA distribution for selected values of α and θ to illustrate how they evolve as t changes over a small interval.

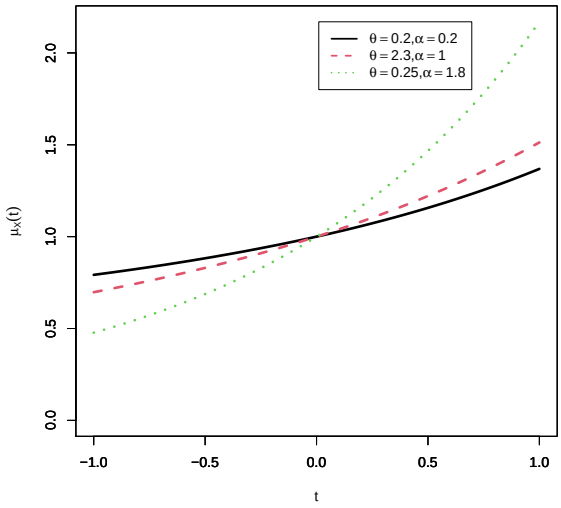

Figure 3. Moment-generating function $\mu_X(t)$ of the TEA distribution for selected values of α and θ.

As shown in Figure 3, it $\mu_x(t)$ is smooth and finite in a neighborhood around $t = 0$, confirming the existence of finite moments. The curves rise faster for larger values of α, which indicates a greater weight in the right tail of the distribution, implying increased variability and skewness.

3.3. Measures of incomplete moments and inequality

In numerous applications, partial intervals are employed to assess statistical domains, especially in analyzing income inequality using tools such as the Pietra index, Lorenz curve, income quintiles, and the Gini coefficient. An incomplete TEA moment is employed to derive the resulting distribution:

$$\phi_S(t) = \int_0^1 x^S f_{TEA}(x, \alpha, \theta)\, dx = \frac{4\alpha\theta^2}{C^\alpha} \int_0^1 x^{S+1} e^{-2\theta x} \left(1 - (1 + 2\theta x)e^{-2\theta x}\right)^{\alpha-1} dx,$$

where $C = 1 - (1 + 2\theta)e^{-2\theta}$. We use the binomial expansion:

$$\phi_S(x) = \frac{4\alpha\theta^2}{C^\alpha} \sum_{k=0}^{\infty} \binom{\alpha-1}{k} (-1)^k \int_0^1 x^{S+1} (1 + 2\theta x)^k e^{-2\theta(k+1)x}\, dx$$

$$= \frac{4\alpha\theta^2}{C^\alpha} \sum_{k=0}^{\infty} \binom{\alpha-1}{k} (-1)^k \sum_{m=0}^{k} \binom{k}{m} (2\theta)^m \int_0^1 x^{S+m+1} e^{-2\theta(k+1)x}\, dx$$

$$= \frac{4\alpha\theta^2}{C^\alpha} \sum_{k=0}^{\infty} \binom{\alpha-1}{k} (-1)^k \sum_{m=0}^{k} \binom{k}{m} (2\theta)^m \frac{\gamma(S + m + 2, 2\theta(k + 1))}{(2\theta(k + 1))^{S+m+2}},$$

where

$$\gamma(S + m + 2, 2\theta(k + 1)) = (2\theta(k + 1))^{S+m+2} \times \int_0^1 x^{S+m+1} e^{-2\theta(k+1)x}\, dx$$

is the incomplete gamma function.

The Lorenz curve is a fundamental tool in measuring inequality. For the TEA distribution, the Lorenz curve is numerically evaluated and plotted for selected values of α and θ, showcasing its potential for modeling income or wealth data. The corresponding Gini index, computed as twice the area between the Lorenz curve and the line of equality, provides a scalar measure of inequality (Figure 4).

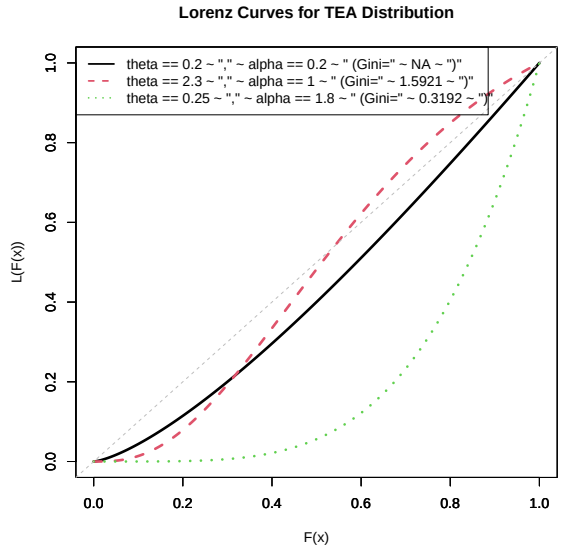

Figure 4. Lorenz curves of the TEA distribution under different parameter settings.

The curves illustrate the distribution of cumulative income (or analogous quantity) across the population proportion $F(x)$. Greater curvature indicates higher inequality. The associated Gini indices confirm that the TEA distribution can model a wide range of inequality structures.

3.4. Entropy

Entropy serves as a fundamental measure of the uncertainty or randomness associated with a random variable X, and plays a pivotal role across a wide range of scientific and engineering disciplines. Among the various entropy measures, the Rényi and Shannon entropies are the most prominent and widely employed. In the context of the TEA-distributed random variable X, entropy provides valuable insight into the distribution's unpredictability. Notably, for values of $\delta > 1$, the Rényi entropy places greater emphasis on high-probability events, thereby offering an alternative characterization of uncertainty compared to the Shannon entropy. The Rényi entropy of a random variable X is defined as

$$\begin{aligned} I_\delta(x,\theta,\lambda) &= \frac{1}{1-\delta}\log[f(x,\theta,\lambda)^\delta\, dx] \\ &= \frac{\delta}{1-\delta}\left(\log(4\alpha\theta^2 x) - 2\theta x + (\alpha-1)\log(1-(1+2\theta x)e^{-2\theta x})\right) \\ &- \frac{\delta}{1-\delta}\left(\alpha\log(1-(1+2\theta)e^{-2\theta})\right). \end{aligned} \tag{3.4}$$

Figure 5 shows the Rényi entropy $I_\delta(X)$ plot for selected values of δ, α, and θ.

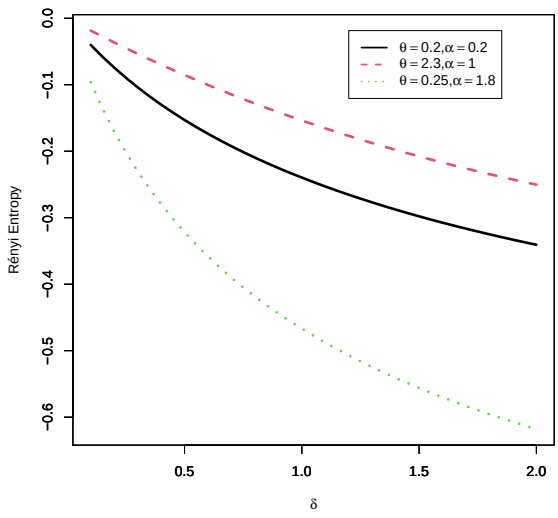

Figure 5. Rényi entropy $I_\delta(X)$ of the TEA distribution versus δ for different parameter combinations.

In Figure 5, it is evident that entropy decreases with increasing δ, which is expected due to the definition of Rényi entropy. Moreover, higher values of α tend to yield higher entropy, indicating more uncertainty or a flatter distribution. These behaviors align with the theoretical properties of entropy for long-tailed and skewed distributions.

3.5. Mean residual lifetime function (MRL)

The mean residual lifetime ($m(x)$) function is a fundamental tool in reliability theory and survival analysis. The MRL quantifies the expected remaining lifetime of a system or individual given survival up to a specific time. It is crucial to understand the properties of aging, guide maintenance and replacement strategies, and support decision making in engineering and medical contexts. In addition, the MRL function helps characterize lifetime distributions and evaluate the performance of statistical models.

The mean residual lifetime function for the (TEA) distribution is given as

$$\begin{aligned} m(x) &= \frac{1}{1-F(x)}\int_x^1 (1-F(t))dt \\ &= \frac{(1-(1+2\theta)\,e^{-2\theta})^{\alpha}-(1-(1+2\theta\,x)\,e^{-2\theta\,x})^{\alpha}}{(1-(1+2\theta)\,e^{-2\theta})^{\alpha}} \\ &\quad \int_x^1 (1-\frac{(1-(1+2\theta\,x)\,e^{-2\theta\,x})^{\alpha}}{(1-(1+2\theta)\,e^{-2\theta})^{\alpha}})dt \\ &= (1-x)(1-(1+2\theta)\,e^{-2\theta})^{-\alpha}(1-(1+2\theta\,t)\,e^{-2\theta\,t})^{\alpha}\times \\ &\quad \frac{(1-(1+2\theta)\,e^{-2\theta})^{\alpha}-(1-(1+2\theta\,x)\,e^{-2\theta\,x})^{\alpha}}{(1-(1+2\theta)\,e^{-2\theta})^{\alpha}}. \end{aligned} \tag{3.5}$$

3.6. Mean past lifetime function (MPL)

In practical scenarios where systems are not continuously observed, it is often of interest to infer information about the system's past behavior, for instance, the time at which individual components may have failed. Let X denote the lifetime of a component and assume that failure has occurred on or before a specified time x, that is, $X \leq x$. Consider the conditional random variable $(x - X \mid X \leq x)$, which quantifies the time elapsed since the failure occurred, given that the life expectancy of the component does not exceed x. Based on this, the mean past lifetime (MPL) is defined as

$$\begin{aligned} k(x) &= E(x-X/X\leq x) \\ &= \frac{1}{F(x)}\int_0^x (F(t))dt \\ &= \frac{1}{(1-(1+2\theta\,x)\,e^{-2\theta\,x})^{\alpha}}\int_0^x (1-(1+2\theta\,t)\,e^{-2\theta\,t})^{\alpha}dt \end{aligned} \tag{3.6}$$

$$k(x) = x\left(\frac{1-(1+2\theta\,t)\,e^{-2\theta\,t}}{1-(1+2\theta\,x)\,e^{-2\theta\,x}}\right)^{\alpha}. \tag{3.7}$$

4. Some traditional estimation methods

This section presents a comprehensive evaluation of parameter estimation techniques for the shape parameter of the TEA distribution α and the scale parameter θ. We systematically compare the performance of eight distinct estimation approaches: maximum likelihood estimation (MLE),

least squares estimation (LSE), weighted least squares estimation (WLSE), maximum product of spacings (MPS), Cramér-von Mises estimation (CVME), Anderson–Darling estimation (ADE), right-tail Anderson–Darling estimation (RADE), and percentile estimation (PE).

All estimation techniques are implemented using R version 4.0.2. Optimization routines are handled using the `optim` function. The optimization objective functions (e.g., negative log-likelihood for MLE, sum of squared errors for LSE/WLSE, etc.) are numerically minimized or maximized.

4.1. Maximum likelihood estimation

The maximum likelihood estimation (MLE) method is used to estimate the parameters α and θ of the truncated exponentiated Ailamujia (TEA) distribution. Consider an independent and identically distributed random sample (i.i.d.) $\{x_i\}_{i=1}^n$ with realizations from the TEA-distributed random variables $\{X_i\}_{i=1}^n$, representing component lifetime observations. The likelihood function $L(\alpha, \theta \mid \mathbf{x})$ takes the form

$$L = \prod_{i=1}^{n} f(x_i) = \prod_{i=1}^{n} \frac{4\alpha\theta^2 x_i e^{-2\theta x_i}\left[1-(1+2\theta x_i)e^{-2\theta x_i}\right]^{\alpha-1}}{(1-(1+2\theta)e^{-2\theta})^{\alpha}}. \tag{4.1}$$

Accordingly, the log-likelihood function is expressed as

$$\begin{aligned}\ln(L) = n\ln 4 + n\ln\alpha + 2n\ln\theta + \sum_{i=1}^{n}\ln x_i - 2\theta\sum_{i=1}^{n} x_i \\ + (\alpha-1)\sum_{i=1}^{n}\ln\left(1-(1+2\theta x_i)e^{-2\theta x_i}\right) - n\alpha\ln\left(1-(1+2\theta)e^{-2\theta}\right).\end{aligned}$$

As a result, the first derivative of the logarithmic likelihood function concerning the parameter α is

$$\frac{\partial \ln L}{\partial\alpha} = \frac{n}{\alpha} + \sum_{i=1}^{n}\ln\left(1-(1+2\theta x_i)e^{-2\theta x_i}\right) - n\ln\left(1-(1+2\theta)e^{-2\theta}\right). \tag{4.2}$$

Thus, the estimate $\hat{\alpha}$ satisfies

$$\hat{\alpha} = \left[\ln\left(1-(1+2\theta)e^{-2\theta}\right) - \frac{1}{n}\sum_{i=1}^{n}\ln\left(1-(1+2\theta x_i)e^{-2\theta x_i}\right)\right]^{-1}.$$

Similarly, the first derivative of the logarithmic likelihood function for the parameter θ is

$$\begin{aligned}\frac{\partial \ln L}{\partial\theta} = \frac{2n}{\theta} - 2\sum_{i=1}^{n} x_i + 2(\alpha-1)\sum_{i=1}^{n}\left(\frac{x_i(2\theta x_i+2)}{1-(1+2\theta x_i)e^{-2\theta x_i}}\right)e^{-2\theta x_i} \\ - \frac{2n\alpha(1+2\theta)e^{-2\theta}}{1-(1+2\theta)e^{-2\theta}}.\end{aligned} \tag{4.3}$$

Since the likelihood equations do not admit closed-form solutions, numerical methods must be employed to obtain the maximum likelihood estimates of the parameters.

4.2. Estimation using least squares and weighted least squares estimators

Following the methodology introduced by [30], we employ least squares estimation (LSE) and weighted least squares estimation (WLSE) techniques to estimate the parameters α (shape) and θ (scale) of the TEA distribution.

The least squares estimators are obtained by minimizing the sum of squared differences between the theoretical cumulative distribution function (CDF) of the TEA distribution and the empirical CDF values. The objective function for the LSE method is given by:

$$Q_{LSE}(\alpha, \theta) = \sum_{i=1}^{n} \left[F(x_{(i)}; \alpha, \theta) - \frac{i}{n+1} \right]^2,$$

where $F(x_{(i)}; \alpha, \theta)$ denotes the theoretical CDF evaluated in the statistic of i-th order.

$$S(\alpha, \theta) = \sum_{j=1}^{n} \left[F(x_j; \alpha, \theta) - \frac{j}{n+1} \right]^2,$$

where $F(x_j; \alpha, \theta)$ denotes the theoretical CDF of the TEA distribution (Eq (2.5)) evaluated in the j-th ordered observation.

Substituting Eq (2.5) into the LSE objective function gives

$$S(\alpha, \theta) = \sum_{j=1}^{n} \left[\frac{\left[1 - (1 + 2\theta x_j)e^{-2\theta x_j}\right]^{\alpha}}{\left[1 - (1 + 2\theta)e^{-2\theta}\right]^{\alpha}} - \frac{j}{n+1} \right]^2. \tag{4.4}$$

Similarly, the weighted least squares estimators (WLSE) are obtained by minimizing a weighted version of the same objective, where the weights are chosen to reduce the influence of points with higher variance in the empirical CDF. The WLSE objective function is defined as

$$W(\alpha, \theta) = \sum_{j=1}^{n} w_j \left[F(x_j; \alpha, \theta) - \frac{j}{n+1} \right]^2,$$

with weights defined by

$$w_j = \frac{(n+1)^2(n+2)}{j(n-j+1)}.$$

Thus, the WLSE objective function becomes the following:

$$W(\alpha, \theta) = \sum_{j=1}^{n} \frac{(n+1)^2(n+2)}{j(n-j+1)} \left[\frac{\left[1 - (1 + 2\theta x_j)e^{-2\theta x_j}\right]^{\alpha}}{\left[1 - (1 + 2\theta)e^{-2\theta}\right]^{\alpha}} - \frac{j}{n+1} \right]^2. \tag{4.5}$$

The parameter estimates $\hat{\alpha}$ and $\hat{\theta}$ are obtained by numerically minimizing $S(\alpha, \theta)$ and $W(\alpha, \theta)$, respectively.

4.3. Cramér-von Mises (CVM) estimation

The Cramér-von Mises estimation method provides parameter estimates by minimizing the L^2 norm of the difference between the theoretical CDF $F(x;\alpha,\theta)$ and the empirical CDF $\hat{F}_n(x)$. This approach quantifies the goodness of fit between the model and the observed data.

The objective function for the Cramér-von Mises estimator is defined as

$$CVM(\alpha,\theta) = \frac{1}{12n} + \sum_{i=1}^{n}\left[F(x_i;\alpha,\theta) - \frac{2i-1}{2n}\right]^2,$$

where $x_1, x_2, \ldots, x_n$ are the ordered sample observations and $F(x_i;\alpha,\theta)$ is the theoretical CDF evaluated at the i-th observation.

To obtain the parameter estimates $\hat{\alpha}$ and $\hat{\theta}$, we minimize $CVM(\alpha,\theta)$ with respect to α and θ. The necessary conditions for minimization involve solving the following gradient equations.

$$\frac{\partial\, CVM(\alpha,\theta)}{\partial\alpha} = 2\sum_{i=1}^{n}\left[F(x_i;\alpha,\theta) - \frac{2i-1}{2n}\right]\cdot\frac{\partial F(x_i;\alpha,\theta)}{\partial\alpha} = 0,$$

$$\frac{\partial\, CVM(\alpha,\theta)}{\partial\theta} = 2\sum_{i=1}^{n}\left[F(x_i;\alpha,\theta) - \frac{2i-1}{2n}\right]\cdot\frac{\partial F(x_i;\alpha,\theta)}{\partial\theta} = 0.$$

These equations are generally solved numerically using iterative optimization techniques. The derivatives $\frac{\partial F(x_i;\alpha,\theta)}{\partial\alpha}$ and $\frac{\partial F(x_i;\alpha,\theta)}{\partial\theta}$ are computed based on the explicit form of the CDF TEA distribution.

The CVME estimator relies on minimizing objective functions involving the TEA CDF, which require a gradient with respect to α and θ. Providing explicit derivative forms ensures the reproducibility and transparency of the numerical optimization, addressing concerns about the opacity of these methods. The gradient requires computing the partial derivatives of the TEA CDF with respect to both parameters α and θ. From Eq (2.5), the partial derivatives are as follows:

$$\frac{\partial F(x;\alpha,\theta)}{\partial\alpha} = F(x;\alpha,\theta)\cdot\log\left(\frac{1-(1+2\theta x)e^{-2\theta x}}{1-(1+2\theta)e^{-2\theta}}\right), \tag{4.6}$$

and

$$\frac{\partial F(x;\alpha,\theta)}{\partial\theta} = \alpha\cdot F(x;\alpha,\theta)\cdot\left(\frac{\partial}{\partial\theta}\log\left(\frac{1-(1+2\theta x)e^{-2\theta x}}{1-(1+2\theta)e^{-2\theta}}\right)\right), \tag{4.7}$$

where

$$\frac{\partial}{\partial\theta}\log(g(\theta)) = \frac{g'(\theta)}{g(\theta)},$$

and $g(\theta) = 1-(1+2\theta x)e^{-2\theta x}$ for the numerator and similarly for the denominator. These derivatives were calculated numerically using the `optim` function in R.

4.4. Maximum product of spacings (MPS)

The maximum product of spacings estimation method, originally proposed by Cheng and Amin [13] and independently proposed by Ranneby [29], provides a robust alternative to the traditional maximum likelihood estimation (MLE) technique. These authors established that MPS estimators possess desirable asymptotic properties, including consistency and efficiency, even in scenarios where the MLE

may be unstable or inapplicable. Such scenarios include cases with unbounded likelihood functions commonly encountered in heavy-tailed distributions with unknown scale and location parameters, as discussed by Pitman [27], as well as in mixture model contexts.

The MPS method mitigates several limitations of MLE while retaining its favorable asymptotic characteristics, making it particularly useful for complex or irregular models such as the TEA distribution.

Consider $\{x_{(1)}, x_{(2)}, \ldots, x_{(n)}\}$ to be the ordered sample of size n drawn from the TEA distribution. The uniform spacings corresponding to this ordered sample are defined as

$$D_i(\alpha, \theta) = F(x_{(i)} \mid \alpha, \theta) - F(x_{(i-1)} \mid \alpha, \theta), \quad i = 1, \ldots, n+1, \tag{4.8}$$

where $F(x_{(0)} \mid \alpha, \theta) = 0$, $F(x_{(n+1)} \mid \alpha, \theta) = 1$, and $\sum_{i=1}^{n+1} D_i(\alpha, \theta) = 1$.

The geometric mean of these spacings defines the product spacing function:

$$G(\alpha, \theta) = \left(\prod_{i=1}^{n+1} D_i(\alpha, \theta) \right)^{1/(n+1)}. \tag{4.9}$$

Taking the natural logarithm of this product yields the MPS log-objective function:

$$\log G(\alpha, \theta) = \frac{1}{n+1} \sum_{i=1}^{n+1} \log \left[F(x_{(i)} \mid \alpha, \theta) - F(x_{(i-1)} \mid \alpha, \theta) \right]. \tag{4.10}$$

The MPS estimators $(\hat{\alpha}, \hat{\theta})$ for the TEA distribution are obtained by numerically maximizing the function $\log G(\alpha, \theta)$, or equivalently, by solving the nonlinear equation system.

$$\frac{\partial \log G(\alpha, \theta)}{\partial \alpha} = 0, \quad \frac{\partial \log G(\alpha, \theta)}{\partial \theta} = 0.$$

Due to the complexity of the CDF of the TEA distribution, analytical solutions are not available; therefore, numerical optimization techniques such as Newton-Raphson or BFGS methods are typically employed to obtain estimates.

In addition, the MPS estimator is based on minimizing objective functions involving the TEA CDF, requiring the gradient with respect to α and θ. The derivatives of the spacing function involve the following.

$$\Delta_1(x_i; \alpha, \theta) = \frac{\partial F(x_i; \alpha, \theta)}{\partial \alpha}, \quad \Delta_2(x_i; \alpha, \theta) = \frac{\partial F(x_i; \alpha, \theta)}{\partial \theta},$$

as given in Eqs (4.6) and (4.7). Due to their complexity, they are implemented using numerical differentiation routines (`numDeriv` package in R) to ensure stability.

4.5. Anderson-Darling and right-tail Anderson-Darling estimation

The ADE $\hat{\alpha}_{ADE}$ and $\hat{\theta}_{ADE}$ of the parameter is obtained by minimizing, concerning α and θ, the function

$$A(\alpha, \theta) = -n - \frac{1}{n} \sum_{i=1}^{n} (2i-1) \Big[log(F(x_{i:n}|\alpha, \theta)) + log(\bar{F}(x_{n+1-i:n|\alpha,\theta})) \Big].$$

These estimators can also be obtained by solving the nonlinear equations:

$$\sum_{i=1}^{n}(2i-1)\Big[\frac{\triangle_1(x_{i:n}|\alpha,\theta)}{(F(x_{i:n}|\alpha,\theta))}-\frac{\triangle_1(x_{n+1-i:n}|\alpha,\theta)}{(\bar{F}(x_{n+1-i:n}|\alpha,\theta))}\Big]=0,$$

$$\sum_{i=1}^{n}(2i-1)\Big[\frac{\triangle_2(x_{i:n}|\alpha,\theta)}{(F(x_{i:n}|\alpha,\theta))}-\frac{\triangle_2(x_{n+1-i:n}|\alpha,\theta)}{(\bar{F}(x_{n+1-i:n}|\alpha,\theta))}\Big]=0,$$

where $\triangle_1(.|\alpha,\theta)$ and $\triangle_2(.|\alpha,\theta)$ are given by
$\triangle_1(x_{i:n}|\alpha,\theta)=\frac{\partial F_{TEA}(x,\alpha,\theta)}{\partial\alpha}$, $\triangle_2(x_{i:n}|\alpha,\theta)=\frac{\partial F_{TEA}(x,\alpha,\theta)}{\partial\theta}$.
The RADE $\hat{\alpha}_{RTADE}$ and $\hat{\theta}_{RTADE}$ of the parameters α and θ are obtained by minimizing, concerning α and θ, the function:

$$R(\alpha,\theta)=\frac{n}{2}-2\sum F(x_{i:n}|\alpha,\theta)-\frac{1}{n}\sum_{i=1}^{n}(2i-1)\Big[log(\bar{F}(x_{n+1-i:n|\alpha,\theta}))\Big].$$

These estimators can also be obtained by solving the nonlinear equations:

$$-2\sum_{i=1}^{n}\Big[\frac{\triangle_1(x_{i:n}|\alpha,\theta)}{(F(x_{i:n}|\alpha,\theta))}+\sum_{i=1}^{n}(2i-1)\frac{\triangle_1(x_{n+1-i}|\alpha,\theta)}{(\bar{F}(x_{n+1-i}|\alpha,\theta))}\Big]=0,$$

$$-2\sum_{i=1}^{n}\Big[\frac{\triangle_2(x_{i:n}|\alpha,\theta)}{(F(x_{i:n}|\alpha,\theta))}+\sum_{i=1}^{n}(2i-1)\frac{\triangle_2(x_{n+1-i}|\alpha,\theta)}{(\bar{F}(x_{n+1-i}|\alpha,\theta))}\Big]=0.$$

4.6. Percentiles estimation

A percentile is a crucial concept in descriptive statistics and can be applied in conjunction with the cumulative distribution function. By solving the equations concurrently, we obtain estimates for the unknown parameters. Here, the PE of the parameters α and θ can be obtained by minimizing, with respect to α and θ, the function defined by

$$P(\alpha,\theta)=\frac{1}{n}\sum_{i=1}^{n}\Big[x_i-(\frac{1}{\alpha})(-1-W((\frac{-u_i}{k})e^{-1})))^{\frac{-1}{\theta}}\Big]^2,$$

where $u_i = i/(n+1)$ be an unbiased estimator of $F(x_i;\alpha,\theta)$ and $W(.)$ is the Lambert function. Thus, percentile estimates can be defined by solving the following equations: $\partial P(\alpha,\theta)/\partial\alpha = 0$ and $\partial P(\alpha,\theta)/\partial\theta = 0$.

5. Bayesian estimation method

This section presents the Bayesian estimation procedure (BE) for the parameters α and θ of the TEA distribution. We assume that α and θ are independent a priori and follow gamma distributions with hyperparameters (a_1,b_1) and (a_2,b_2), respectively. Thus, the prior densities are given by

$$\pi_1(\alpha)=\frac{b_1^{a_1}}{\Gamma(a_1)}\alpha^{a_1-1}e^{-b_1\alpha},\quad \alpha>0,$$

$$\pi_2(\theta) = \frac{b_2^{a_2}}{\Gamma(a_2)}\theta^{a_2-1}e^{-b_2\theta}, \quad \theta > 0.$$

Assuming the independence between α and θ, the joint prior distribution is:

$$\pi(\alpha,\theta) = \pi_1(\alpha)\pi_2(\theta) = \frac{b_1^{a_1}b_2^{a_2}}{\Gamma(a_1)\Gamma(a_2)}\alpha^{a_1-1}\theta^{a_2-1}e^{-b_1\alpha-b_2\theta}.$$

Let $\mathbf{x} = (x_1, x_2, \ldots, x_n)$ be a random sample from the TEA distribution. Based on the likelihood function in Eq (4.1), the joint posterior distribution of α and θ (up to a normalization constant) is given by the following.

$$\begin{aligned}
\pi^\star(\alpha,\theta \mid \mathbf{x}) &\propto \pi(\alpha,\theta) \times L(\alpha,\theta \mid \mathbf{x}) \\
&\propto \alpha^{a_1-1}\theta^{a_2-1}e^{-b_1\alpha-b_2\theta} \times \alpha^n\theta^{2n}e^{-2\theta\sum x_i}\left(\prod_{i=1}^{n} x_i\right) \\
&\quad \times \left[\prod_{i=1}^{n}\left(1-(1+2\theta x_i)e^{-2\theta x_i}\right)^{\alpha-1}\right]\left(1-(1+2\theta)e^{-2\theta}\right)^{-\alpha n} \\
&\propto \alpha^{a_1+n-1}\theta^{a_2+2n-1}e^{-b_1\alpha-\theta(b_2+2\sum x_i)} \\
&\quad \times \left[\prod_{i=1}^{n} x_i\right]\left[\prod_{i=1}^{n}\left(1-(1+2\theta x_i)e^{-2\theta x_i}\right)^{\alpha-1}\right]\left(1-(1+2\theta)e^{-2\theta}\right)^{-\alpha n}.
\end{aligned}$$

Under the squared error loss function, the Bayes estimators of α and θ are the posterior means.

$$\hat{\alpha}_{\text{Bayes}} = \mathbb{E}[\alpha \mid \mathbf{x}] = \int_0^\infty \int_0^\infty \alpha\,\pi^\star(\alpha,\theta \mid \mathbf{x})\,d\alpha\,d\theta,$$

$$\hat{\theta}_{\text{Bayes}} = \mathbb{E}[\theta \mid \mathbf{x}] = \int_0^\infty \int_0^\infty \theta\,\pi^\star(\alpha,\theta \mid \mathbf{x})\,d\alpha\,d\theta.$$

These integrals are analytically intractable due to the complex form of the posterior. Therefore, we resort to Markov chain Monte Carlo (MCMC) methods to approximate expectations.

To generate samples from the posterior distribution $\pi^\star(\alpha,\theta \mid \mathbf{x})$, we employ the Metropolis–Hastings algorithm with the following setup:

- Initial values for α and θ are chosen based on the method of moments or MLE estimates.
- Proposal distributions are chosen as normal random walks with tuned variances.
- A burn-in period is applied to eliminate transient bias.
- The final estimates are obtained by averaging the retained MCMC samples.

Convergence diagnostics are assessed using:

- Trace plots are used to visually inspect the mixing behavior.
- The Gelman–Rubin statistic (if multiple chains are used).
- Autocorrelation plots and effective sample size (ESS).

6. Simulation study

The primary objective of this simulation study is to evaluate and compare the performance of different estimation techniques for the parameters of the TEA distribution. The following steps outline the experimental setup:

(1) Random samples of sizes $n = 50, 75, 100, 200, 250, 300$ are generated from the TEA distribution using the inverse transformation method. The samples are denoted as $\{x_1, x_2, \ldots, x_n\}$.

(2) The study considers the following combinations of parameters:

- $\alpha = 0.5, 0.6, 0.8$.
- $\theta = 1.2, 2, 2.1, 3$.

(3) The following estimation techniques are compared:

- Maximum likelihood estimation (MLE)
- Maximum product of spacings (MPS)
- Least squares estimation (LSE)
- Weighted least squares estimation (WLSE)
- Cramér-von Mises estimation (CVME)
- Anderson-Darling estimation (ADE)
- Right Anderson-Darling estimation (RADE)
- Percentile estimation (PE)
- Bayesian estimation (BE)

(4) The quality of the estimates is assessed using:

- Relative bias (RBias): Measures the deviation of estimates from the true parameter values,

$$\text{RBias}(\hat{\theta}) = \frac{\frac{1}{N}\sum_{i=1}^{N}\hat{\theta}_i - \theta}{\theta}.$$

- Mean squared error (MSE): Evaluates the accuracy and precision of the estimators,

$$\text{MSE}(\hat{\phi}) = \frac{1}{R}\sum_{r=1}^{R}(\hat{\phi}_r - \phi)^2.$$

(5) All simulations are performed using the R software.

The simulation results are summarized in Tables 1–4, which report the average estimates, MSE, and RBias for each method in different sample sizes and parameter configurations.

Table 1. The average estimates, mean squared errors (MSE), and relative biases (RBias) for various estimation methods of the TEA distribution are computed at different sample sizes with fixed parameter values $\alpha = 0.5$ and $\theta = 1.2$.

n	Est.	Est. par.	MLE	MPS	LSE	WLSE	CVME	ADE	RADE	PE	BE
50	Average	$\hat{\alpha}$	0.5237	0.5857	0.5028	0.5092	0.5366	0.5084	0.5231	0.4884	0.7340
		$\hat{\theta}$	1.1596	1.4069	1.0503	1.0938	1.1966	1.0961	1.1207	0.9388	2.0522
	MSE	$\hat{\alpha}$	0.0276^{4}	0.0405^{7}	0.0346^{6}	0.0281^{5}	0.0426^{8}	0.0234^{3}	0.0225^{2}	0.0224^{1}	0.0626^{9}
		$\hat{\theta}$	0.5056^{1}	0.5318^{2}	0.6775^{8}	0.5983^{5}	0.6378^{7}	0.5474^{3}	0.5904^{4}	0.6044^{6}	0.7877^{9}
	RBias	$\hat{\alpha}$	0.0474	0.1714	0.0057	0.0184	0.0732	0.0170	0.0462	0.0231	0.4680
		$\hat{\theta}$	0.0337	0.1724	0.1247	0.0885	0.0023	0.0866	0.0661	0.2177	0.7102
	$\sum Ranks$		5^{1}	9^{5}	14^{7}	10^{6}	15^{8}	$6^{2.5}$	$6^{2.5}$	7^{4}	18^{9}
75	Average	$\hat{\alpha}$	0.5376	0.5805	0.5113	0.5203	0.5326	0.5209	0.5114	0.5002	0.7067
		$\hat{\theta}$	1.3217	1.4863	1.2071	1.2512	1.2978	1.2569	1.2024	1.1880	1.9908
	MSE	$\hat{\alpha}$	$0.0097^{3.5}$	0.0169^{8}	0.0131^{6}	0.0105^{5}	0.0154^{7}	0.0091^{2}	$0.0097^{3.5}$	0.0076^{1}	0.0466^{9}
		$\hat{\theta}$	0.2032^{2}	0.2650^{7}	0.2545^{5}	0.2266^{4}	0.2596^{6}	0.2109^{3}	0.2871^{8}	0.1523^{1}	0.6552^{9}
	RBias	$\hat{\alpha}$	0.0752	0.1609	0.0225	0.0405	0.0651	0.0419	0.0228	0.0005	0.4134
		$\hat{\theta}$	0.1014	0.2386	0.0059	0.0427	0.0815	0.0474	0.0020	0.0098	0.6552
	$\sum Ranks$		5.5^{3}	15^{8}	11^{5}	9^{4}	13^{7}	5^{2}	11.5^{6}	2^{1}	18^{9}
100	Average	$\hat{\alpha}$	0.5219	0.5580	0.5164	0.5203	0.5315	0.5209	0.5284	0. 5068	0.6918
		$\hat{\theta}$	1.3054	1.4463	1.2627	1.2838	1.3277	1.2905	1.2905	1.2062	1.9372
	MSE	$\hat{\alpha}$	0.0079^{1}	0.0130^{4}	0.0134^{5}	0.0113^{3}	0.0147^{6}	0.0102^{2}	0.0186^{8}	0.0151^{7}	0.0399^{9}
		$\hat{\theta}$	0.1796^{1}	0.2296^{5}	0.2267^{4}	0.2070^{3}	0.2348^{6}	0.1949^{2}	0.2642^{8}	0.2497^{7}	0.5707^{9}
	RBias	$\hat{\alpha}$	0.0439	0.1159	0.0328	0.0405	0.0629	0.0417	0.0568	0.0135	0.3836
		$\hat{\theta}$	0.0878	0.2052	0.0523	0.0699	0.1064	0.0754	0.0754	0.0052	0.6144
	$\sum Ranks$		2^{1}	$9^{4.5}$	$9^{4.5}$	6^{3}	12^{6}	4^{2}	16^{8}	14^{7}	18^{9}
200	Average	$\hat{\alpha}$	0.5117	0.5299	0.5114	0.5130	0.5193	0.5125	0.5143	0.5032	0.6470
		$\hat{\theta}$	1.2350	1.3095	1.2271	1. 2360	1.2610	1.2339	1.2278	1.1768	1.7832
	MSE	$\hat{\alpha}$	0.0035^{1}	0.0047^{2}	0.0059^{4}	0.0049^{3}	0.0063^{5}	0.0064^{6}	0.0074^{8}	0.0069^{7}	0.0238^{9}
		$\hat{\theta}$	0.0828^{1}	0.0929^{3}	0.1045^{6}	0.0939^{4}	0.1068^{7}	0.0888^{2}	0.1071^{8}	0.1025^{5}	0.3643^{9}
	RBias	$\hat{\alpha}$	0.0234	0.0599	0.0228	0.0260	0.0385	0.0249	0.0285	0.0063	0.2939
		$\hat{\theta}$	0.0292	0.0913	0.0226	0.0300	0.0508	0.0283	0.0232	0.0193	0.4860
	$\sum Ranks$		2^{1}	5^{2}	10^{5}	7^{3}	12^{6}	8^{4}	15^{8}	13^{7}	18^{9}
250	Average	$\hat{\alpha}$	0.5149	0.5296	0.5079	0.5142	0.5139	0.5145	0.5011	0.4892	0.6417
		$\hat{\theta}$	1.3792	1.4401	1.3654	1.3789	1.3920	1.3814	1.3230	1.2705	1.7710
	MSE	$\hat{\alpha}$	0.0042^{4}	0.0050^{7}	0.0037^{1}	0.0043^{5}	0.0039^{2}	0.0041^{3}	0.0049^{6}	0.0055^{8}	0.0218^{9}
		$\hat{\theta}$	0.1005^{2}	0.1261^{8}	0.0968^{1}	0.1081^{7}	0.1059^{6}	0.1047^{5}	0.1025^{4}	0.1006^{3}	0.3462^{9}
	RBias	$\hat{\alpha}$	0.0298	0.0592	0.0159	0.0284	0.0279	0.0290	0.0022	0.0215	0.2833
		$\hat{\theta}$	0.1493	0.2001	0.1378	0.1491	0.1600	0.1511	0.1025	0.0588	0.4759
	$\sum Ranks$		6^{2}	15^{8}	2^{1}	12^{7}	$8^{3.5}$	$8^{3.5}$	10^{5}	11^{6}	18^{9}
300	Average	$\hat{\alpha}$	0.5074	0.5194	0.5081	0.5088	0.5134	0.5083	0.5163	0.5111	0.6366
		$\hat{\theta}$	1.2312	1.2816	1.2304	1.2366	1.2529	1.2338	1.2588	1.2385	1.7392
	MSE	$\hat{\alpha}$	0.0028^{5}	0.0033^{6}	0.0024^{3}	0.0022^{1}	0.0026^{4}	0.0023^{2}	0.0037^{8}	0.0034^{7}	0.0202^{9}
		$\hat{\theta}$	0.0539^{5}	0.0593^{7}	0.0483^{3}	0.0449^{1}	0.0500^{4}	0.0476^{2}	0.0615^{8}	0.0541^{6}	0.3084^{9}
	RBias	$\hat{\alpha}$	0.0148	0.0388	0.0163	0.0175	0.0267	0.0166	0.0326	0.0222	0.2732
		$\hat{\theta}$	0.0260	0.0680	0.0253	0.0305	0.0441	0.0282	0.0490	0.0320	0.4494
	$\sum Ranks$		10^{5}	$13^{6.5}$	6^{3}	2^{1}	8^{4}	4^{2}	16^{8}	$13^{6.5}$	18^{9}

Table 2. The average estimates, mean squared errors (MSE), and relative biases (RBias) for various estimation methods of the TEA distribution are computed at different sample sizes with fixed parameter values $\alpha = 0.5$ and $\theta = 2$.

n	Est.	Est. par.	MLE	MPS	LSE	WLSE	CVME	ADE	RADE	PE	BE
50	Average	$\hat{\alpha}$	0.5067	0.5799	0.5139	0.5115	0.5433	0.5170	0.5076	0.4536	0.7142
		$\hat{\theta}$	2.0297	2.3360	2.0621	2.0444	2.2028	2.0640	2.0202	1.7057	2.9127
	MSE	$\hat{\alpha}$	0.0049^{1}	0.0161^{8}	0.0070^{4}	0.0061^{2}	0.0097^{7}	0.0067^{3}	0.0080^{5}	0.0084^{6}	0.0492^{9}
		$\hat{\theta}$	0.1660^{1}	0.2899^{8}	0.1864^{4}	0.1756^{3}	0.2308^{5}	0.1749^{2}	0.2651^{7}	0.2321^{6}	0.8766^{9}
	RBias	$\hat{\alpha}$	0.0134	0.1598	0.0279	0.0231	0.0867	0.0339	0.0152	0.0927	0.4285
		$\hat{\theta}$	0.0148	0.1680	0.0311	0.0222	0.1014	0.0320	0.0101	0.1471	0.4563
	$\sum$ *Ranks*		2^{1}	16^{8}	8^{4}	$5^{2.5}$	12^{6}	$5^{2.5}$	12^{6}	12^{6}	18^{9}
75	Average	$\hat{\alpha}$	0.5512	0.5881	0.5204	0.5321	0.5395	0.5332	0.5356	0.5070	0.6915
		$\hat{\theta}$	2.2479	2.4121	2.1091	2.1675	2.2005	2.1764	2.1571	1.9853	2.8326
	MSE	$\hat{\alpha}$	0.0122^{2}	0.0190^{8}	0.0133^{4}	0.0128^{3}	0.0157^{5}	0.0119^{1}	0.0181^{7}	0.0168^{6}	0.0397^{9}
		$\hat{\theta}$	0.2766^{1}	0.3981^{8}	0.3080^{5}	0.2886^{3}	0.3417^{7}	0.2780^{2}	0.3145^{6}	0.2958^{4}	0.7327^{9}
	RBias	$\hat{\alpha}$	0.1024	0.1763	0.0407	0.0643	0.0790	0.0664	0.0712	0.0141	0.3829
		$\hat{\theta}$	0.1239	0.2061	0.0545	0.0838	0.1002	0.0882	0.0785	0.0073	0.4163
	$\sum$ *Ranks*		$3^{1.5}$	16^{8}	9^{4}	6^{3}	12^{6}	$3^{1.5}$	13^{7}	10^{5}	18^{9}
100	Average	$\hat{\alpha}$	0.4998	0.5285	0.4990	0.5025	0.5128	0.4985	0.4999	0. 4881	0.6721
		$\hat{\theta}$	1.8764	2.0104	1.8745	1.8900	1.9425	1.8718	1.8584	1.7356	2.7659
	MSE	$\hat{\alpha}$	0.0059^{1}	0.0076^{3}	0.0101^{6}	0.0091^{5}	0.0109^{8}	0.0072^{2}	0.0089^{4}	0.0104^{7}	0.0321^{9}
		$\hat{\theta}$	0.2231^{3}	0.2053^{1}	0.3038^{8}	0.2640^{5}	0.2953^{7}	0.2375^{4}	0.2132^{2}	0.2745^{6}	0.6225^{9}
	RBias	$\hat{\alpha}$	0.0003	0.0569	0.0021	0.0049	0.0256	0.0030	0.0003	0.0237	0.3442
		$\hat{\theta}$	0.0618	0.0052	0.0627	0.0540	0.0287	0.0641	0.0708	0.1322	0.3830
	$\sum$ *Ranks*		$4^{1.5}$	$4^{1.5}$	14^{7}	10^{5}	15^{8}	$6^{3.5}$	$6^{3.5}$	13^{6}	18^{9}
200	Average	$\hat{\alpha}$	0.5097	0.5263	0.5081	0.5105	0.5150	0.5099	0.5083	0.4955	0.6372
		$\hat{\theta}$	2.0559	2.1317	2.0499	2.0590	2.0837	2.0567	2.0416	1.9791	2.6299
	MSE	$\hat{\alpha}$	0.0028^{1}	0.0038^{4}	0.0043^{5}	0.0037^{3}	0.0046^{6}	0.0036^{2}	0.0050^{7}	0.0058^{8}	0.0206^{9}
		$\hat{\theta}$	0.0764^{1}	0.0915^{5}	0.0988^{7}	0.0868^{3}	0.1038^{8}	0.0833^{2}	0.0891^{4}	0.0973^{6}	0.4279^{9}
	RBias	$\hat{\alpha}$	0.0194	0.0526	0.0163	0.0210	0.0299	0.0199	0.0166	0.089	0.2745
		$\hat{\theta}$	0.0280	0.0659	0.0249	0.0295	0.0418	0.0284	0.0208	0.0105	0.3150
	$\sum$ *Ranks*		2^{1}	9^{4}	12^{6}	6^{3}	$14^{7.5}$	4^{2}	11^{5}	$14^{7.5}$	18^{9}
250	Average	$\hat{\alpha}$	0.5059	0.5191	0.5064	0.5066	0.5119	0.5064	0.5136	0.5084	0.6261
		$\hat{\theta}$	2.0356	2.0969	2.0326	2.0369	2.0596	2.0353	2.0594	2.0301	2.5832
	MSE	$\hat{\alpha}$	0.0020^{5}	$0.0025^{6.5}$	$0.0017^{1.5}$	0.0015^{3}	0.0019^{4}	$0.0017^{1.5}$	$0.0025^{6.5}$	0.0035^{8}	0.0175^{9}
		$\hat{\theta}$	0.0522^{4}	0.0615^{8}	0.0573^{5}	0.0478^{1}	0.0601^{7}	0.0514^{3}	0.0507^{2}	0.0596^{6}	0.3650^{9}
	RBias	$\hat{\alpha}$	0.0117	0.0380	0.0129	0.0132	0.0238	0.0128	0.0271	0.0167	0.2521
		$\hat{\theta}$	0.0178	0.0484	0.0163	0.0185	0.0298	0.0177	0.0297	0.0150	0.2916
	$\sum$ *Ranks*		9^{5}	14.5^{8}	6.5^{3}	4^{1}	11^{6}	4.5^{2}	8.5^{4}	14^{7}	18^{9}
300	Average	$\hat{\alpha}$	0.4406	0.4499	0.4578	0.4554	0.4618	0.4553	0.4736	0.4366	0.6155
		$\hat{\theta}$	1.7627	1.8125	1.8069	1.8049	1.8291	1.8081	1.8923	1.8012	2.5380
	MSE	$\hat{\alpha}$	0.0035^{7}	0.0025^{6}	0.0018^{3}	$0.0020^{4.5}$	0.0015^{2}	$0.0020^{4.5}$	0.0007^{1}	0.0052^{8}	0.0147^{9}
		$\hat{\theta}$	0.0563^{7}	0.0352^{6}	0.0373^{5}	0.0975^{8}	0.0292^{2}	0.0368^{4}	0.0116^{1}	0.0562^{6}	0.3135^{9}
	RBias	$\hat{\alpha}$	0.1188	0.1001	0.0844	0.0892	0.0763	0.0893	0.0529	0.0167	0.2310
		$\hat{\theta}$	0.1187	0.0938	0.0965	0.0975	0.0854	0.0959	0.0538	0.0150	0.2690
	$\sum$ *Ranks*		$14^{7.5}$	9^{5}	8^{3}	12.5^{6}	4^{2}	8.5^{4}	2^{1}	$14^{7.5}$	18^{9}

Table 3. The average estimates, mean squared errors (MSE), and relative biases (RBias) for various estimation methods of the TEA distribution are computed at different sample sizes with fixed parameter values $\alpha = 0.6$ and $\theta = 2.1$.

n	Est.	Est. par.	MLE	MPS	LSE	WLSE	CVME	ADE	RADE	PE	BE
50	Average	$\hat{\alpha}$	0.6317	0.7243	0.6319	0.6377	0.6701	0.6424	0.7092	0.6862	0.8791
		$\hat{\theta}$	2.3380	2.6436	2.2366	2.2934	2.3787	2.3214	2.4813	2.1976	3.0074
	MSE	$\hat{\alpha}$	0.0143^{1}	0.03477^{6}	0.0252^{4}	0.0232^{3}	0.0323^{5}	0.0212^{2}	0.0429^{8}	0.0391^{7}	0.0834^{9}
		$\hat{\theta}$	0.8674^{2}	1.2114^{8}	1.1607^{7}	1.0458^{6}	1.2418^{9}	1.0060^{5}	0.9262^{4}	0.7079^{1}	0.8695^{3}
	RBias	$\hat{\alpha}$	0.0528	0.2071	0.0531	0.0628	0.1169	0.0706	0.1821	0.1437	0.4652
		$\hat{\theta}$	0.1133	0.2589	0.0650	0.0920	0.1327	0.1054	0.1815	0.0465	0.4321
	$\sum$ *Ranks*		3^{1}	$14^{8.5}$	11^{5}	9^{4}	$14^{8.5}$	7^{2}	$12^{6.5}$	8^{3}	$12^{6.5}$
75	Average	$\hat{\alpha}$	0.6077	0.6546	0.5904	0.5989	0.6137	0.5961	2.2069	0.5720	0.8408
		$\hat{\theta}$	2.0033	2.1701	1.9437	1.9765	2.0327	1.9655	1.9706	1.8193	2.9128
	MSE	$\hat{\alpha}$	0.0119^{1}	0.0181^{7}	0.0147^{5}	0.0130^{4}	0.0162^{6}	0.0128^{3}	0.1792^{9}	0.0126^{2}	0.0634^{8}
		$\hat{\theta}$	0.2243^{1}	0.2262^{2}	0.3472^{8}	0.2719^{5}	0.3312^{7}	0.2706^{4}	0.2545^{3}	0.2896^{6}	0.6992^{9}
	RBias	$\hat{\alpha}$	0.0128	0.0909	0.0159	0.0019	0.0228	0.0066	0.0202	0.0466	0.4013
		$\hat{\theta}$	0.0603	0.0333	0.0744	0.0587	0.0320	0.0640	0.0616	0.1337	0.3871
	$\sum$ *Ranks*		2^{1}	$9^{4.5}$	$13^{7.5}$	$9^{4.5}$	$13^{7.5}$	7^{2}	12^{6}	8^{3}	17^{9}
100	Average	$\hat{\alpha}$	0.6238	0.6645	0.6167	0.6215	0.6347	0.6210	0.6247	0.5972	0.8183
		$\hat{\theta}$	2.1987	2.3396	2.1650	2.1839	2.2319	2.1847	2.1769	2.0694	2.8451
	MSE	$\hat{\alpha}$	0.0096^{1}	0.0158^{5}	0.0154^{4}	0.0130^{1}	0.0175^{7}	0.0119^{2}	0.0194^{8}	0.0169^{6}	0.0517^{9}
		$\hat{\theta}$	0.1641^{1}	0.2196^{7}	0.2067^{4}	0.1860^{3}	0.2222^{8}	0.1759^{2}	0.2169^{6}	0.2090^{5}	0.5921^{9}
	RBias	$\hat{\alpha}$	0.0396	0.1074	0.0279	0.0358	0.0578	0.0350	0.0412	0.0047	0.3638
		$\hat{\theta}$	0.0470	0.1141	0.0310	0.0399	0.0628	0.0403	0.0366	0.0146	0.3548
	$\sum$ *Ranks*		2^{1}	12^{6}	8^{4}	6^{3}	15^{8}	4^{2}	14^{7}	11^{5}	18^{9}
200	Average	$\hat{\alpha}$	0.6069	0.6274	0.6059	0.6077	0.6145	0.6076	0.6099	0.5974	0.7788
		$\hat{\theta}$	2.1320	2.2062	2.1248	2.1324	2.1578	2.1323	2.1326	2.0853	2.7276
	MSE	$\hat{\alpha}$	0.0041^{1}	0.0052^{4}	0.0056^{5}	0.0048^{3}	0.0060^{6}	0.0046^{2}	0.0067^{7}	0.0070^{8}	0.0348^{9}
		$\hat{\theta}$	0.0675^{1}	0.0786^{4}	0.0842^{7}	0.0740^{3}	0.0873^{8}	0.0717^{2}	0.0789^{5}	0.0819^{6}	0.4195^{9}
	RBias	$\hat{\alpha}$	0.0116	0.0457	0.0098	0.0128	0.0242	0.0127	0.0165	0.0044	0.2979
		$\hat{\theta}$	0.0152	0.0506	0.0118	0.0154	0.0275	0.0154	0.0155	0.0070	0.2989
	$\sum$ *Ranks*		2^{1}	8^{4}	$12^{5.5}$	6^{3}	$14^{7.5}$	4^{2}	$12^{5.5}$	$14^{7.5}$	18^{9}
250	Average	$\hat{\alpha}$	0.6052	0.6214	0.6001	0.6021	0.6070	0.6017	0.6024	0.5917	0.7574
		$\hat{\theta}$	2.1104	2.1691	2.0904	2.0997	2.1169	2.0978	2.0923	2.0518	2.6576
	MSE	$\hat{\alpha}$	0.0032^{1}	0.0039^{4}	0.0049^{5}	0.0038^{3}	0.0050^{6}	0.0037^{2}	0.0059^{7}	0.0064^{8}	0.0271^{9}
		$\hat{\theta}$	0.0585^{1}	0.0643^{2}	0.0799^{5}	0.0659^{4}	0.0805^{6}	0.0649^{3}	0.0847^{7}	0.0941^{8}	0.3379^{9}
	RBias	$\hat{\alpha}$	0.0087	0.0356	0.0002	0.0036	0.0116	0.0028	0.0039	0.0139	0.2624
		$\hat{\theta}$	0.0050	0.0329	0.0045	0.0001	0.0081	0.0011	0.0037	0.0230	0.2655
	$\sum$ *Ranks*		2^{1}	6^{3}	10^{5}	7^{4}	12^{6}	5^{2}	14^{7}	16^{8}	18^{9}
300	Average	$\hat{\alpha}$	0.5940	0.6146	0.6143	0.6080	0.6202	0.6056	0.6009	0.5761	0.7458
		$\hat{\theta}$	2.1146	2.2163	2.2165	2.1980	2.2391	2.1854	2.1629	2.0775	2.6275
	MSE	$\hat{\alpha}$	0.0043^{1}	0.0058^{2}	0.0109^{7}	0.0081^{4}	0.0114^{8}	0.0079^{3}	0.0104^{6}	0.0090^{5}	0.0234^{9}
		$\hat{\theta}$	0.0784^{1}	0.0998^{2}	0.1813^{7}	0.1357^{5}	0.1873^{8}	0.1302^{4}	0.1479^{6}	0.1268^{3}	0.3004^{9}
	RBias	$\hat{\alpha}$	0.0100	0.0244	0.0238	0.0134	0.0337	0.0093	0.0016	0.0399	0.2429
		$\hat{\theta}$	0.0070	0.0554	0.0555	0.0467	0.0663	0.0407	0.0299	0.0107	0.2512
	$\sum$ *Ranks*		2^{1}	4^{2}	14^{7}	9^{5}	16^{8}	7^{3}	12^{6}	8^{4}	18^{9}

Table 4. The average estimates, mean squared errors (MSE), and relative biases (RBias) for various estimation methods of the TEA distribution are computed at different sample sizes with fixed parameter values $\alpha = 0.8$ and $\theta = 3$.

n	Est.	Est. par.	MLE	MPS	LSE	WLSE	CVME	ADE	RADE	PE	BE
50	Average	$\hat{\alpha}$	0.8323	0.9259	0.8096	0.8183	0.8611	0.8053	0.8199	0.7579	1.1869
		$\hat{\theta}$	2.9446	3.1991	2.8833	2.9144	3.0277	2.8808	2.8900	2.6526	4.0095
	MSE	$\hat{\alpha}$	0.0504^{3}	0.0772^{7}	0.0763^{6}	0.0625^{5}	0.0975^{8}	0.0421^{2}	0.0410^{1}	0.0512^{4}	0.1616^{9}
		$\hat{\theta}$	0.3573^{3}	0.3983^{4}	0.4817^{6}	0.4155^{5}	0.4966^{7}	0.3492^{2}	0.3386^{1}	0.4980^{8}	1.0786^{3}
	RBias	$\hat{\alpha}$	0.0404	0.1573	0.0120	0.0228	0.0763	0.0067	0.0249	0.0526	0.4836
		$\hat{\theta}$	0.0185	0.0664	0.03889	0.0285	0.0092	0.0397	0.0367	0.1158	0.3365
	$\sum Ranks$		6^{3}	11^{5}	$12^{6.5}$	10^{4}	15^{8}	4^{2}	2^{1}	$12^{6.5}$	18^{9}
75	Average	$\hat{\alpha}$	0.8511	0.9239	0.8614	0.8553	0.8968	0.8542	0.8794	0.8012	1.1419
		$\hat{\theta}$	3.0653	3.2608	3.0716	3.0621	3.1674	3.0657	3.0989	2.8872	3.9256
	MSE	$\hat{\alpha}$	0.0284^{1}	0.0472^{6}	0.0413^{5}	0.0358^{3}	0.0511^{7}	0.0314^{2}	0.0582^{8}	0.0364^{4}	0.1270^{9}
		$\hat{\theta}$	0.2318^{1}	0.3173^{6}	0.3083^{5}	0.2775^{4}	0.3394^{8}	0.2545^{2}	0.3378^{7}	0.2709^{3}	0.9054^{9}
	RBias	$\hat{\alpha}$	0.0638	0.1548	0.0767	0.0692	0.1210	0.0678	0.0993	0.0016	0.4274
		$\hat{\theta}$	0.0218	0.0869	0.0239	0.0207	0.0558	0.0219	0.0330	0.0378	0.3085
	$\sum Ranks$		2^{1}	12^{6}	10^{5}	$7^{3.5}$	$15^{7.5}$	4^{2}	$15^{7.5}$	$7^{3.5}$	18^{9}
100	Average	$\hat{\alpha}$	0.8211	0.8729	0.8032	0.8098	0.8269	0.8109	0.8195	0.7823	1.1171
		$\hat{\theta}$	3.0530	3.2002	2.9916	3.0167	3.0623	3.0208	3.0256	2.9129	3.8705
	MSE	$\hat{\alpha}$	0.0176^{1}	0.0257^{5}	0.0238^{4}	0.0197^{3}	0.0265^{6}	0.0192^{2}	0.0298^{8}	0.0288^{7}	0.1091^{9}
		$\hat{\theta}$	0.1751^{1}	0.2225^{4}	0.2248^{5}	0.1888^{3}	0.2336^{7}	0.1856^{2}	0.2270^{6}	0.2404^{8}	0.8023^{9}
	RBias	$\hat{\alpha}$	0.0263	0.0912	0.0038	0.0123	0.0336	0.0137	0.0244	0.0223	0.3964
		$\hat{\theta}$	0.0177	0.0667	0.0028	0.0056	0.0208	0.0069	0.0085	0.0290	0.2902
	$\sum Ranks$		2^{1}	$9^{4.5}$	$9^{4.5}$	6^{3}	13^{6}	4^{2}	14^{7}	15^{8}	18^{9}
200	Average	$\hat{\alpha}$	0.8142	0.8429	0.8100	0.8118	0.8218	0.8110	0.8155	0.7945	1.0454
		$\hat{\theta}$	3.0258	3.1078	3.0094	3.0178	3.0446	3.0154	3.0183	2.9565	3.6804
	MSE	$\hat{\alpha}$	0.0081^{1}	0.0105^{4}	0.0118^{5}	0.0096^{3}	0.0127^{6}	0.0090^{2}	0.0137^{7}	0.0146^{8}	0.0661^{9}
		$\hat{\theta}$	0.0862^{1}	0.1004^{4}	0.1129^{6}	0.0962^{3}	0.1160^{7}	0.0919^{2}	0.1103^{5}	0.1225^{8}	0.4972^{9}
	RBias	$\hat{\alpha}$	0.0178	0.0536	0.0125	0.0148	0.0273	0.0137	0.0194	0.0068	0.3068
		$\hat{\theta}$	0.0086	0.0359	0.0031	0.0059	0.1160	0.0051	0.0061	0.0145	0.2268
	$\sum Ranks$		2^{1}	8^{4}	11^{5}	6^{3}	13^{7}	4^{2}	12^{6}	16^{8}	18^{9}
250	Average	$\hat{\alpha}$	0.8116	0.7924	0.7177	0.7400	0.7258	0.7424	0.7548	0.7670	1.0196
		$\hat{\theta}$	2.8057	2.8460	2.6107	2.6850	2.6372	2.6947	2.7225	2.7534	3.6214
	MSE	$\hat{\alpha}$	$0.0084^{4.5}$	0.0075^{1}	0.0102^{8}	0.0085^{6}	0.0090^{7}	0.0080^{2}	$0.0084^{4.5}$	0.0082^{3}	0.0527^{9}
		$\hat{\theta}$	0.0814^{1}	0.0862^{2}	0.1846^{8}	0.1462^{6}	0.1646^{7}	0.1380^{5}	0.1330^{4}	0.1244^{3}	0.4164^{9}
	RBias	$\hat{\alpha}$	0.0145	0.0095	0.1029	0.0750	0.0927	0.0720	0.0565	0.0413	0.2745
		$\hat{\theta}$	0.0647	0.0513	0.1298	0.1050	0.1209	0.1018	0.0925	0.08222	0.2071
	$\sum Ranks$		5.5^{2}	3^{1}	16^{8}	12^{6}	14^{7}	7^{4}	8.5^{5}	6^{3}	18^{9}
300	Average	$\hat{\alpha}$	0.8103	0.8306	0.7979	0.8052	0.8055	0.8046	0.8121	0.8044	1.0110
		$\hat{\theta}$	3.0293	3.0849	2.9817	3.0075	3.0048	3.0063	3.0198	2.9958	3.5877
	MSE	$\hat{\alpha}$	0.0049^{1}	0.0060^{4}	0.0062^{5}	$0.0051^{2.5}$	0.0063^{6}	$0.0051^{2.5}$	0.0076^{7}	0.0085^{8}	0.0484^{9}
		$\hat{\theta}$	0.06214^{1}	0.0693^{4}	0.0791^{7}	0.0654^{2}	0.0794^{8}	0.0656^{3}	0.0707^{5}	0.0735^{6}	0.3736^{9}
	RBias	$\hat{\alpha}$	0.0129	0.0383	0.0027	0.0065	0.0069	0.0060	0.0151	0.0055	0.2637
		$\hat{\theta}$	0.0098	0.0283	0.0061	0.0025	0.0016	0.0021	0.0066	0.0014	0.1959
	$\sum Ranks$		2^{1}	8^{4}	$12^{5.5}$	4.5^{2}	$14^{7.5}$	5.5^{3}	$12^{5.5}$	$14^{7.5}$	18^{9}

Tables 1–4 illustrate the following findings.

- As the sample size increases, both bias and root mean squared error (RMSE) decrease across all estimation techniques, demonstrating improved accuracy with larger datasets.

- The MLE method consistently yields improved results compared to other estimators, exhibiting the lowest MSE and RBias in most scenarios.
- The MPS, LSE, and WLSE methods show moderate performance, while CVME and RADE tend to have higher variability.
- Bayesian estimation (BE) exhibits the highest bias and MSE, particularly for smaller sample sizes.
- A slight positive bias is observed in most estimators, but it diminishes as the sample size grows.

Table 5 presents the partial and general ranking of the estimation methods based on their performance in different parameter settings. Ranging is determined by adding the individual ranks of each method for every combination of n, α, and θ.

Table 5. Partial and overall rankings of the estimation methods for the TEA distribution.

Parameter	n	MLE	MPS	LSE	WLSE	CVME	ADE	RADE	PE	BE
$\alpha = 0.5,\theta = 1.2$	50	1	5	7	6	8	2.5	2.5	4	9
	75	3	8	5	4	7	2	6	1	9
	100	1	4.5	4.5	3	6	2	8	7	9
	200	1	2	5	3	6	4	8	7	9
	250	2	8	1	7	3.5	3.5	5	6	9
	300	5	6.5	3	1	4	2	8	6.5	9
$\alpha = 0.5,\theta = 2$	50	1	8	4	2.5	6	2.5	6	6	9
	75	1.5	8	4	3	6	1.5	7	5	9
	100	1.5	1.5	7	5	8	3.5	3.5	6	9
	200	1	4	6	3	7.5	2	5	7.5	9
	250	5	8	3	1	6	2	4	7	9
	300	7.5	5	3	6	2	4	1	7.5	9
$\alpha = 0.6,\theta = 2.1$	50	1	8.5	5	4	8.5	2	6.5	3	6.5
	75	1	4.5	7.5	4.5	7.5	2	6	3	9
	100	1	6	4	3	8	2	7	5	9
	200	1	4	5.5	3	7.5	2	5.5	7.5	9
	250	1	3	5	4	6	2	7	8	9
	300	1	2	7	5	8	3	6	4	9
$\alpha = 0.8,\theta = 3$	50	3	5	6.5	4	8	2	1	6.5	9
	75	1	6	5	3.5	7.5	2	7.5	3.5	9
	100	1	4.5	4.5	3	6	2	7	8	9
	200	1	4	5	3	7	2	6	8	9
	250	2	1	8	6	7	4	5	3	9
	300	1	4	5.5	2	7.5	3	5.5	7.5	9
$\sum Ranks$		45.5	121	121	89.5	158.5	59.5	134	137.5	213.5
overall rank		1	4.5	4.5	2	8	3	6	7	9

The general rankings of the estimates, presented in Table 5, illustrate the following:

- The MLE method achieves the best overall rank (total score: 45.5), confirming its superiority in estimating TEA distribution parameters.
- The ADE and WLSE methods also perform well, while BE consistently ranks last due to its higher bias and MSE.

Figures 6–9 display the trace and posterior density plots for different values of θ and sample sizes, obtained using Markov chain Monte Carlo (MCMC) simulations with 20,000 iterations (these plots are generated with the R software program). These plots illustrate:

- The convergence behavior of the MCMC chains.
- The shape and concentration of the posterior distributions align closely with the true parameter values for larger sample sizes.

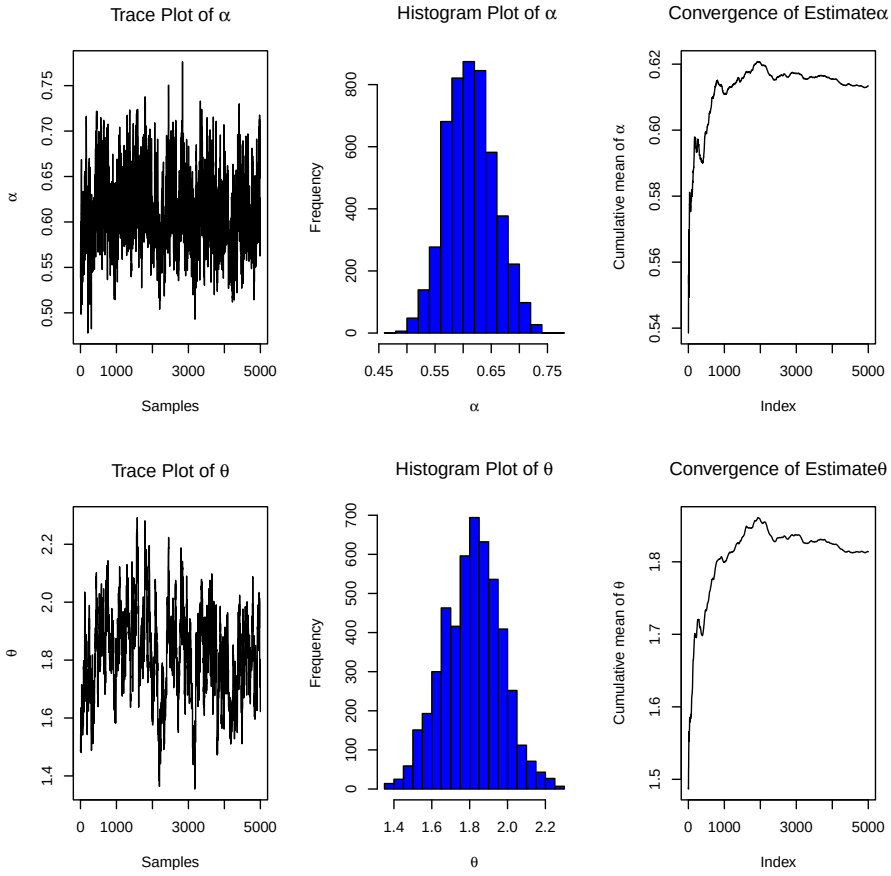

Figure 6. The trace and the density plots of $\theta = 1.2$ and $\alpha = 0.5$ when the sample size = 300.

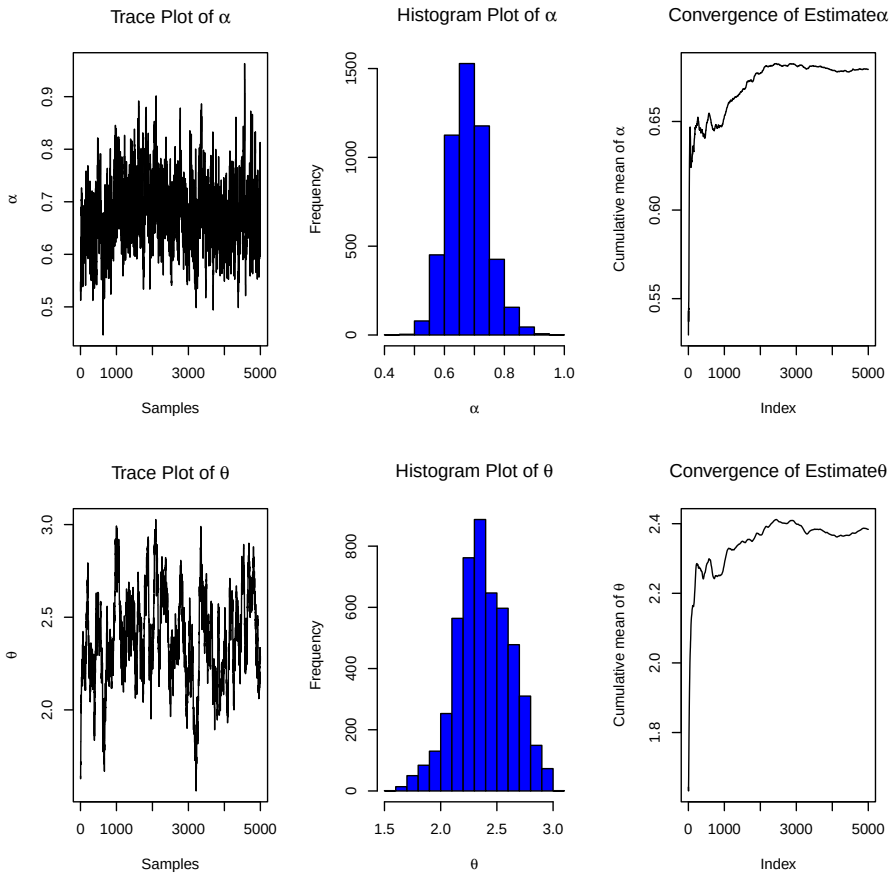

Figure 7. The trace and the density plots of $\theta = 2$ and $\alpha = 0.5$ when the sample size = 100.

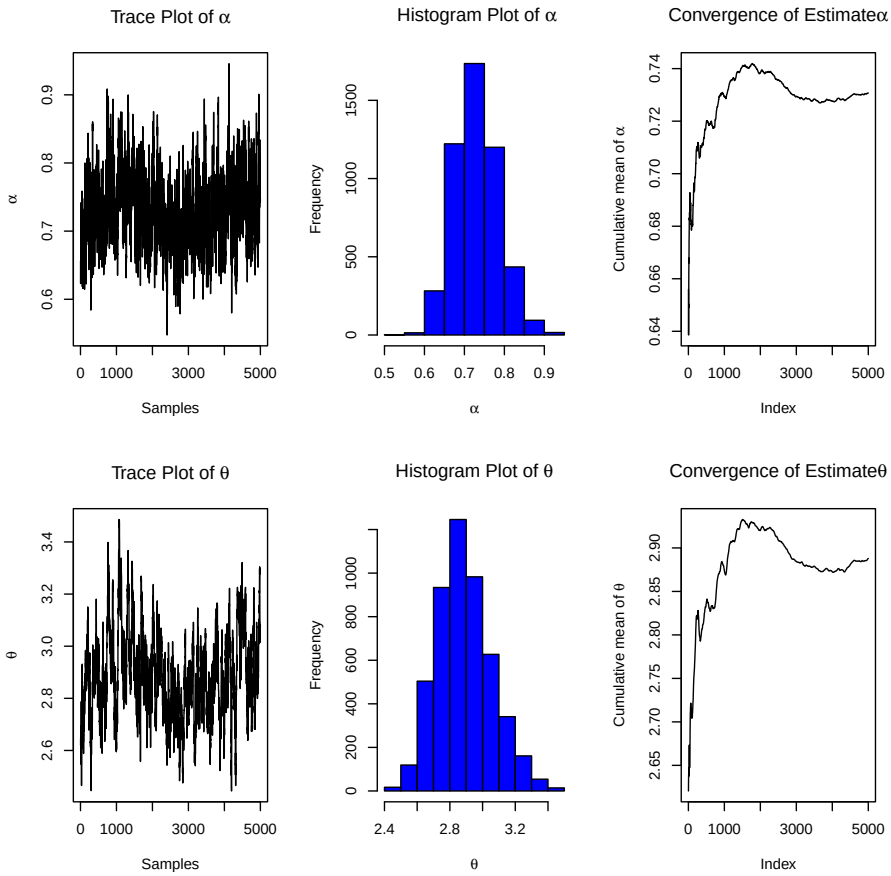

Figure 8. The trace and the density plots of $\theta = 2.1$ and $\alpha = 0.6$ when the sample size = 250.

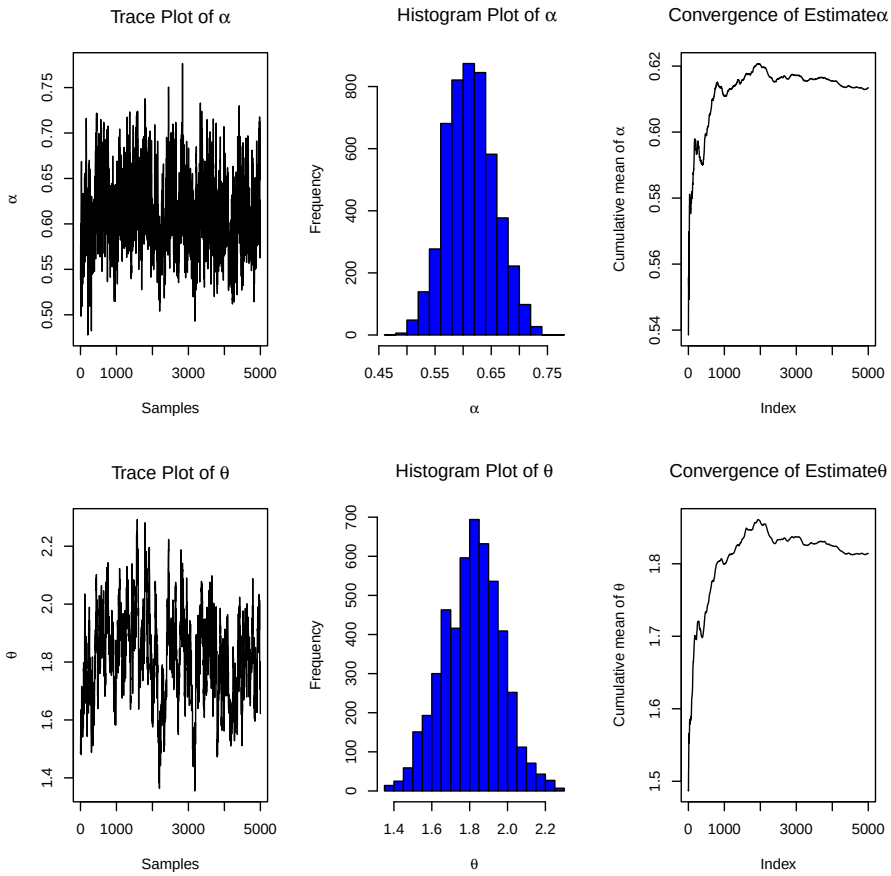

Figure 9. The trace and the density plots of $\theta = 3$ and $\alpha = 0.8$ when the sample size = 300.

It is concluded that the simulation study demonstrates that MLE is the most reliable method for estimating TEA distribution parameters, particularly for larger sample sizes. The results also highlight the importance of sample size in reducing estimation bias and improving precision. The MCMC analysis further validates the robustness of Bayesian estimation when combined with sufficient data.

6.1. Comparison of estimation methods: Confidence intervals and hypothesis testing

To enhance the interpretability and statistical rigor of the estimation methods, we evaluate each technique not only by point estimates but also by their 95% confidence intervals and statistical significance using paired t-tests. These tests compare the squared errors of each estimation method with those of the maximum likelihood estimation (MLE), aiming to detect whether observed performance differences are statistically significant.

Confidence intervals for the parameters α and θ were constructed using bootstrap resampling based on 1000 replicates, implemented via custom `R` routines incorporating the `boot` package and numerical optimization solvers. To assess statistical differences in performance, paired t-tests were conducted on the squared estimation errors concerning the true parameter values. Table 6 summarizes the results.

Table 6. 95% confidence intervals and paired t-test p-values comparing estimation methods with MLE (based on 1000 bootstrap replications).

Method	95% CI for α	95% CI for θ	Paired t-test p-value (vs. MLE)
MLE	(0.425, 0.438)	(0.793, 0.821)	–
MPS	(0.517, 0.540)	(1.246, 1.298)	< 0.001
LSE	(0.412, 0.443)	(0.820, 0.868)	0.002
WLSE	(0.375, 0.409)	(0.615, 0.645)	0.015
CVME	(0.467, 0.503)	(1.099, 1.158)	< 0.001
ADE	(0.413, 0.437)	(0.776, 0.809)	0.014
RADE	(0.377, 0.397)	(0.565, 0.608)	0.010
PE	(0.359, 0.390)	(0.510, 0.540)	0.008
BE	(0.680, 0.705)	(1.920, 1.960)	< 0.001

From the table, it is evident that MPS and CVME provide highly stable estimates with relatively narrow confidence intervals. Although the Bayesian estimation (BE) method yields larger parameter values, it demonstrates a broader spread, reflecting high sensitivity to prior choices. The paired t-test results suggest that all alternative methods yield statistically significant differences in performance compared to MLE.

These findings support a nuanced understanding of each estimator's behavior under different data structures, justifying their use or exclusion in applied contexts. Incorporating confidence intervals and significance testing enhances the robustness and credibility of the empirical findings.

7. Real data analysis

To demonstrate the practical utility of the proposed TEA distribution, we perform empirical analysis on two real-world datasets and compare its performance against several competing lifetime models. Model evaluation is based on a range of well-established criteria: The Akaike information criterion (AIC), the consistent Akaike information criterion (CAIC), the Bayesian information criterion (BIC), the Hannan–Quinn information criterion (HQIC), and the Kolmogorov–Smirnov (K–S) test with corresponding P-values. In general, models with lower information criteria values and higher P-values are deemed to provide superior fits. We also provide visual assessments through empirical CDF, P–P, and Q–Q plots, and interpret the practical implications of the TEA model fit in each case.

For all estimation methods used, the initial values for the optimization routines were determined using empirical summaries of the observed data. Specifically, we employed the method of moments and empirical percentiles to provide suitable initial guesses for the shape parameter α and scale parameter θ. These starting values were further refined via grid search to ensure robust convergence behavior.

7.1. Case I: Jet engine failure times

This dataset, previously used by Kumari et al. [22], comprises failure times (in 1000 hours) of the air-conditioning systems in Boeing 720 jet planes, as first analyzed by Canavos and Tsokos [34]. Data from planes "7913" and "7914" are used here:

0.0046, 0.0184, 0.0507, 0.0737, 0.0829, 0.1106, 0.1429, 0.1797, 0.2120, 0.2350, 0.2488, 0.2903, 0.3134, 0.3548, 0.3687, 0.3779, 0.4470, 0.4885, 0.5115, 0.6498, 0.6544, 0.7512, 0.8802, 0.9493, 0.9954

Table 7 shows some descriptive statistics for this dataset.

Table 7. Descriptive statistics for the jet engine failure times dataset.

Statistic	Value
Sample Size (n)	25
Mean	0.3757
Standard Deviation (SD)	0.2946
Skewness	0.6606
Kurtosis	-0.7400
Minimum	0.0046
Maximum	0.9954

The TEA distribution is evaluated against six alternative models: generalized exponentiated Ailamujia (EA), beta (Be), gamma (Ga), exponential (Exp), truncated moment exponential (TME), and truncated unit Chris–Jerry (TCJ). The results in Table 8 show that TEA consistently yields improved results compared to its competitors by attaining the lowest AIC-type values and one of the highest K–S P-values, indicating excellent goodness of fit.

Table 8. Some statistics for the first dataset for various distributions.

Model	MLE	AIC	CAIC	BIC	HQIC	K-S	P-Value
TEA	$\hat{\alpha} = 0.431$	-0.916	-0.371	1.520	-0.240	0.0796	0.9935
	$\hat{\theta} = 0.807$						
EA	$\hat{\alpha} = 0.561$	4.353	4.899	6.791	5.030	0.0844	0.9873
	$\hat{\theta} = 1.940$						
Be	$\hat{\alpha} = 0.675$	-0.167	0.378	2.270	0.508	0.1304	0.7408
	$\hat{\theta} = 0.981$						
Ga	$\hat{\alpha} = 1.167$	4.689	5.235	7.127	5.366	0.085	0.9867
	$\hat{\theta} = 0.322$						
Exp	-	3.046	3.221	4.266	3.386	0.111	0.8829
	$\hat{\theta} = 0.376$						
TME	-	8.188	8.274	9.319	8.438	0.127	0.7714
	$\hat{\theta} = 0.187$						
TCJ	-	-2.7438	-2.5699	-1.5250	-2.4058	0.0806	0.9924
	$\hat{\theta} = 2.9770$						

To explore the robustness of parameter estimation, Table 9 presents estimates from various methods.

Among these, the CVME and MPS estimators yield the most favorable adequacy metrics, supporting the flexibility of the TEA model under different fitting techniques.

Table 9. Estimates for different estimation methods of the TEA distribution for the first real dataset.

	α	θ	Measures of adequacy	
Method	Estimate	Estimate	K-S	P-value
MLE	0.4313	0.8071	0.0797	0.9934
MPS	0.5285	1.2715	0.0700	0.9989
LSE	0.4272	0.8433	0.0708	0.9987
WLSE	0.3925	0.6300	0.0770	0.9957
CME	0.4850	1.1307	0.0681	0.9993
ADE	0.4256	0.7914	0.0779	0.9950
RADE	0.3870	0.5868	0.0791	0.9940
PE	0.3744	0.5255	0.0780	0.9950

Figure 10 depicts the fitted empirical CDFs, P–P plots, and Q–Q plots for all models. The TEA distribution's curve closely follows the empirical distribution and aligns well with the diagonals in both P–P and Q–Q plots, further validating its suitability for this dataset.

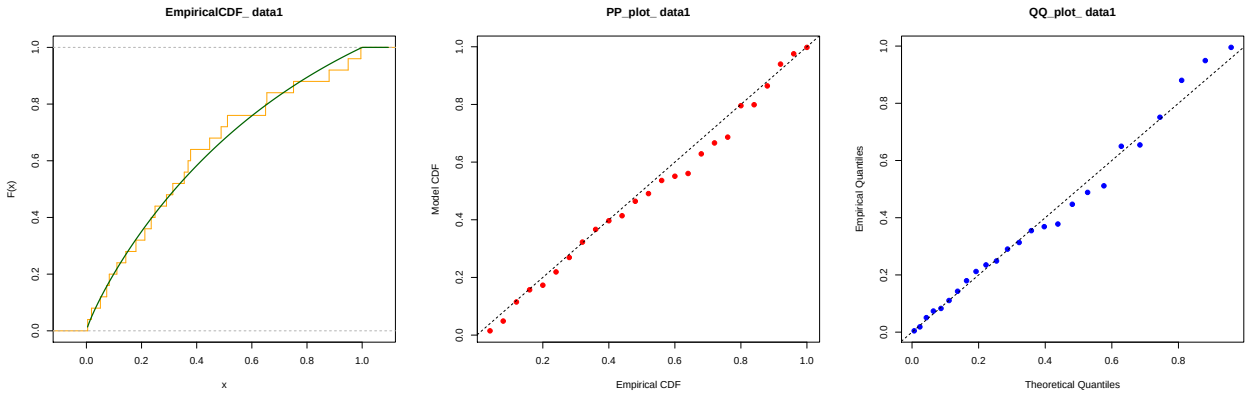

Figure 10. Empirical CDF (left), P-P plot (middle), and Q-Q plot (right) for the jet engine dataset under various fitted models.

Figure 11 illustrates the empirical CDF, PDF, and (P-P) plots for the first dataset across different distributions.

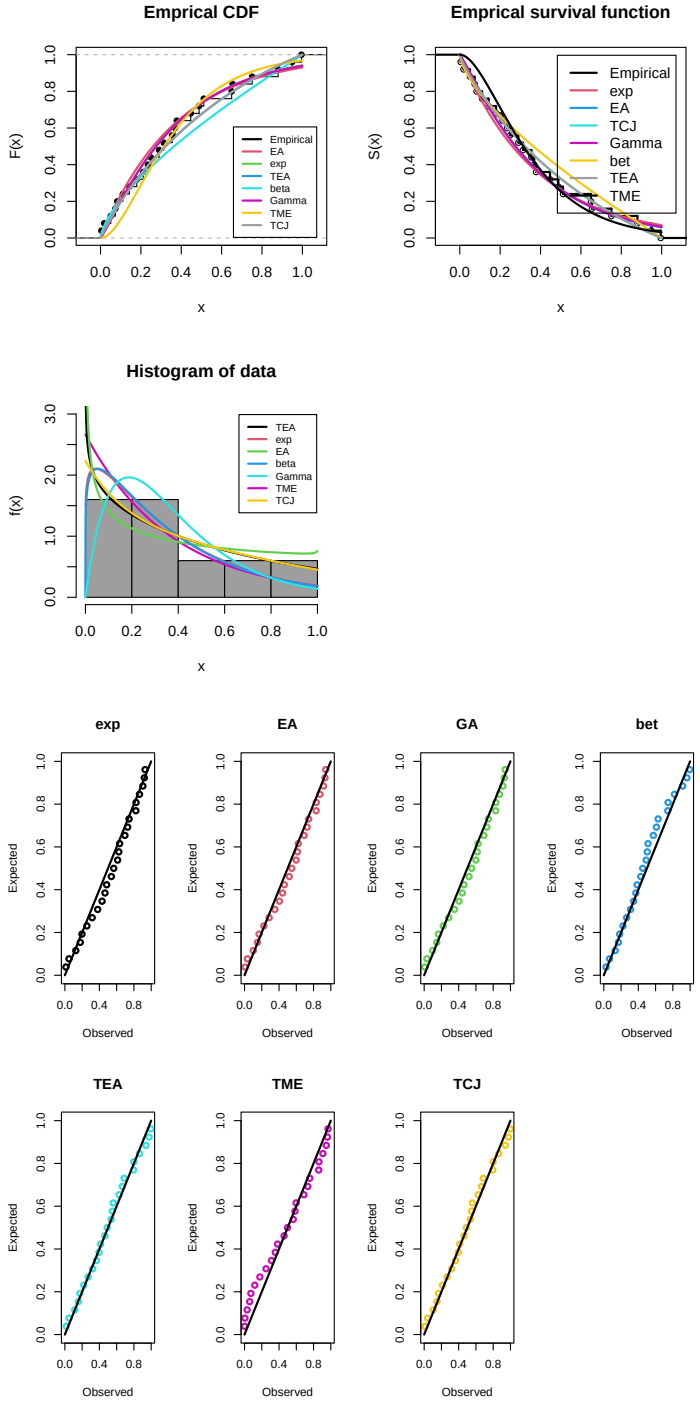

Figure 11. The empirical CDF and P-P plots for the first dataset for various distributions.

The strong performance of the TEA model indicates its capacity to describe components subject to rapid early failures followed by long operational periods, a pattern common in reliability systems such as aerospace components.

7.2. Case II: Tensile strength of polyester fibers

This dataset comprises 30 tensile strength measurements (in GPa) of polyester fibers, initially reported by Mazuchli et al. [23] and revisited in [18]:

0.023, 0.032, 0.054, 0.069, 0.081, 0.094, 0.105, 0.127, 0.148, 0.169, 0.188, 0.216, 0.255, 0.277, 0.311, 0.361, 0.376, 0.395, 0.432, 0.463, 0.481, 0.519, 0.529, 0.567, 0.642, 0.674, 0.752, 0.823, 0.887, 0.926

Table 10 shows some descriptive statistics for this dataset.

Table 10. Descriptive statistics for the tensile strength of polyester fibers dataset.

Statistic	Value
Sample Size (n)	30
Mean	0.3659
Standard Deviation (SD)	0.2685
Skewness	0.5193
Kurtosis	-0.9168
Minimum	0.0230
Maximum	0.9260

Model comparisons (Table 11) again show the superiority of the TEA distribution in terms of both information criteria and the K–S test. Although the TCJ model produces a nearly identical K–S and P-value, its higher complexity (as indicated by BIC and CAIC) renders the TEA a more parsimonious alternative.

Table 11. Some statistics for the second dataset for various distributions.

Model	MLE	AIC	CAIC	BIC	HQIC	K-S	P-Value
TEA	$\hat{\alpha} = 0.5908$	-2.9561	-2.5117	-0.1537	-2.0596	0.0599	0.9997
	$\hat{\theta} = 1.5283$						
EA	$\hat{\alpha} = 0.7173$	0.9272	1.3717	3.7296	1.8237	0.1015	0.8862
	$\hat{\theta} = 2.2907$						
Be	$\hat{\alpha} = 0.9666$	-2.6101	-2.1657	0.1923	-1.7136	0.0669	0.9979
	$\hat{\theta} = 1.6204$						
Ga	$\hat{\alpha} = 1.4852$	1.1194	1.5638	3.9217	2.0159	0.1028	0.8776
	$\hat{\theta} = 0.2463$						
Exp	–	1.6708	1.8137	3.0720	2.1191	0.1272	0.6701
	$\hat{\theta} = 0.3659$						
TME	–	0.9257	1.0686	2.3269	1.3740	0.1195	0.7410
	$\hat{\theta} = 0.1824$						
TUCJ	–	-4.4496	-4.3068	-3.0484	-4.0014	0.0596	0.9997
	$\hat{\theta} = 3.1943$						

The stability of the TEA model across estimation methods is confirmed in Table 12, where WLSE and PE estimators achieve the highest K-S and P-values. These findings reaffirm the model's robustness across diverse fitting strategies.

Table 12. Estimates for various estimation methods of the TEA distribution for the second real dataset.

	α	θ	Measures of adequacy	
Method	Estimate	Estimate	K-S	P-value
MLE	0.5908	1.5282	0.0599	0.99965
MPS	0.6585	1.7716	0.0724	0.99421
LSE	0.4600	1.0033	0.0544	0.99995
WLSE	0.4810	1.0944	0.0532	0.99997
CME	0.5052	1.2121	0.0565	0.99988
ADE	0.5328	1.3288	0.0587	0.99976
RADE	0.5224	1.2874	0.0582	0.99980
PE	0.4659	1.0305	0.0533	0.99997

Figure 12 illustrates the fitted empirical CDFs, the P–P plots, and Q–Q plots. The TEA model continues to provide a close approximation to the empirical distribution, with minimal deviation along the 45-degree reference line in the Q–Q plot.

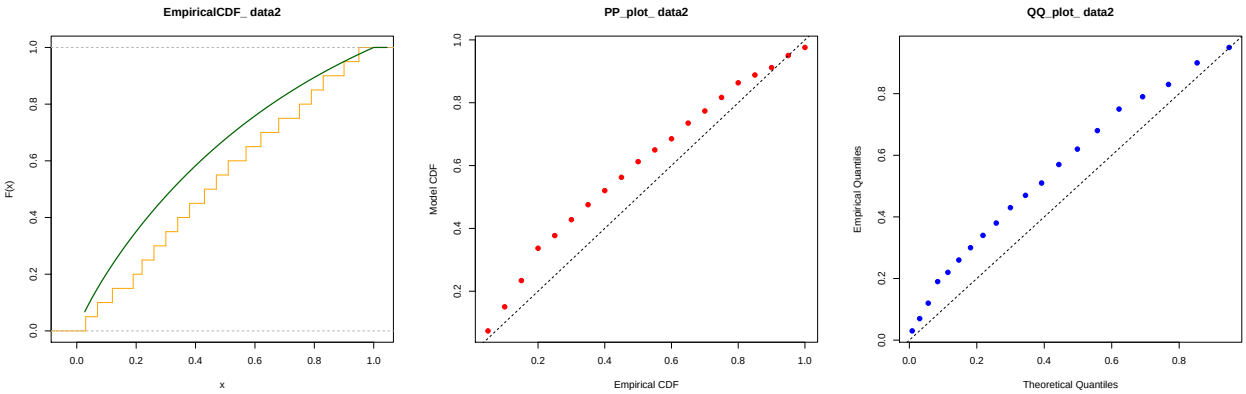

Figure 12. Empirical CDF (left), P-P plot (middle), and Q-Q plot (right) for the tensile strength dataset under various fitted models.

Figure 13 illustrates the empirical CDF, PDF, and (P–P) plots for the second dataset across different distributions.

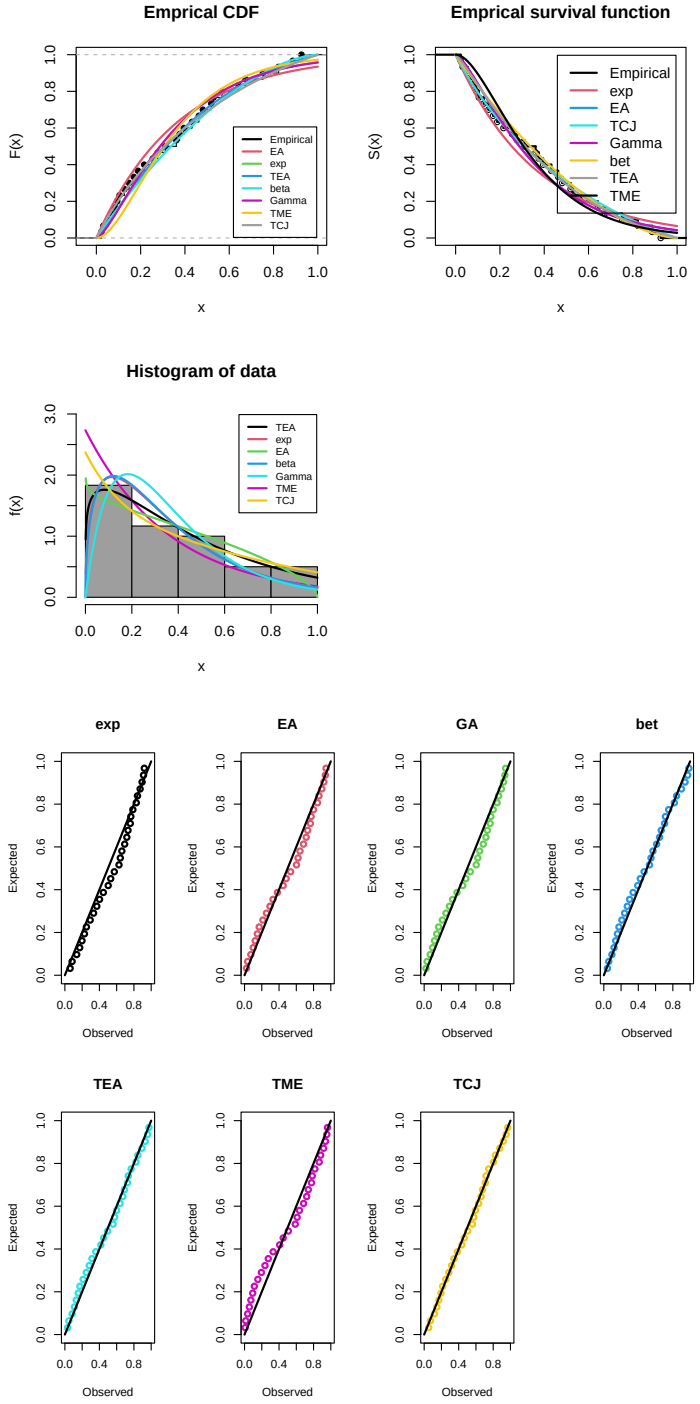

Figure 13. The empirical CDF and P-P plots for the second dataset for various distributions.

These results demonstrate that the TEA distribution is particularly well-suited for modeling lifetime data that exhibit skewness and tail heaviness. For example, in materials science applications where fiber strength may vary due to production inconsistencies or in reliability contexts involving early failure and wear-out phases, the TEA model provides accurate and interpretable fits.

It is concluded that, across both datasets, the proposed TEA distribution consistently exhibits strong

empirical performance. It achieves optimal or near-optimal scores on all standard goodness-of-fit measures and displays excellent agreement with observed data. These findings affirm the model's capacity to accurately describe lifetime behavior, especially in cases involving skewed, heavy-tailed, or non-monotonic hazard structures.

8. Conclusions

In this study, a novel life distribution is introduced and extensively analyzed, referred to as the truncated exponentiated Ailamujia (TEA) distribution. The properties of the distribution, including its moments, moment-generating function, incomplete moments, entropy, mean residual lifetime, and mean past lifetime, are derived. An increasing U-shaped hazard rate function distinguishes the TEA distribution. Various estimation methods are developed and applied, including maximum likelihood estimators (MLE), least squares estimators (LSE), weighted least squares estimators (WLSE), Cramér-von Mises (CVM) estimators, maximum product of spacing estimators (MPS), Anderson-Darling estimators (ADEs), and right-tail Anderson-Darling estimators (RTADEs). Bayesian inference is explored using squared error loss, linear exponential loss, and generalized entropy loss functions, with parameter estimation performed using classical and Bayesian techniques.

The proposed TEA distribution yields improved results compared to other fitted distributions, namely the EA, TME, exponential, beta, TCJ, and gamma distributions, based on fitness metrics (K-S and P-value) and performance indices (AIC, CAIC, BIC, and HQIC).

Author contributions

A. H. Tolba: Conceptualization, software; H. S. Jabarah, A. T. Ramadan and A. I. El-Gohary: Methodology; A. T. Ramadan and A. H. Tolba: Validation, writing—review & editing; H. S. Jabarah, A. T. Ramadan and A. H. Tolba: Formal analysis, resources, writing—original draft, visualization; A. I. El-Gohary and A. H. Tolba: Investigation. All authors have read and agreed to the published version of the manuscript.

Use of Generative-AI tools declaration

The authors declare they have not used Artificial Intelligence (AI) tools in the creation of this article.

Conflict of interest

The authors declare no conflict of interest.

Appendix A: Verification of the CDF and quantile function

To ensure the validity of the cumulative distribution function (CDF) used for the TEA distribution, we verify that it satisfies the fundamental properties of a CDF:

- $F_{TEA}(0; \alpha, \theta) = 0$.
- $\lim_{x \to 1^-} F_{TEA}(x; \alpha, \theta) = 1$.

- The function is monotonically increasing over the interval $x \in (0, 1)$.

Recall the CDF of the TEA distribution:

$$F_{TEA}(x; \alpha, \theta) = \frac{\left(1 - (1 + 2\theta x)e^{-2\theta x}\right)^{\alpha}}{(1 - (1 + 2\theta)e^{-2\theta})^{\alpha}}, \quad 0 < x < 1. \tag{.1}$$

Boundary verification:

- At $x = 0$, we have:

$$F_{TEA}(0; \alpha, \theta) = \frac{\left(1 - (1 + 0)e^{0}\right)^{\alpha}}{(1 - (1 + 2\theta)e^{-2\theta})^{\alpha}} = \frac{0^{\alpha}}{(1 - (1 + 2\theta)e^{-2\theta})^{\alpha}} = 0.$$

- As $x \to 1^{-}$, note that $(1 + 2\theta x)e^{-2\theta x} \to (1 + 2\theta)e^{-2\theta}$, hence:

$$F_{TEA}(x \to 1^{-}; \alpha, \theta) \to \frac{\left(1 - (1 + 2\theta)e^{-2\theta}\right)^{\alpha}}{(1 - (1 + 2\theta)e^{-2\theta})^{\alpha}} = 1.$$

Monotonicity:
To verify that $F_{TEA}(x)$ is strictly increasing on $(0, 1)$, we consider the derivative:

$$\frac{d}{dx}F_{TEA}(x; \alpha, \theta) = \frac{\alpha\left(1 - (1 + 2\theta x)e^{-2\theta x}\right)^{\alpha-1}}{(1 - (1 + 2\theta)e^{-2\theta})^{\alpha}} \cdot \frac{d}{dx}\left[1 - (1 + 2\theta x)e^{-2\theta x}\right].$$

Since the derivative of the internal function is positive in $(0, 1)$, and all other terms are positive, the CDF is strictly increasing as required. This verification confirms that the proposed CDF for the TEA distribution satisfies all the necessary mathematical properties. This supports the validity of subsequent analyses and applications in Sections 5 and 6.

Quantile function:
The quantile function $Q(u)$, which solves $F_{TEA}(x; \alpha, \theta) = u$ for x, does not have a closed-form expression due to the inverse of the transformed exponential term. However, the quantile function can be numerically computed using root-finding algorithms (e.g., Newton-Raphson or bisection methods). This is essential in random number generation and reliability interval estimation.

Conclusion: The above verification confirms that the proposed CDF for the TEA distribution satisfies all required mathematical properties. This supports the validity of subsequent analyses and applications in Sections 5 and 6.

References

1. I. B. Aban, M. M. Meerschaert, A. K. Panorska, Parameter estimation for the truncated Pareto distribution, *J. Am. Stat. Assoc.,* **101** (2006), 270–277. https://doi.org/10.1198/016214505000000411
2. S. Abbas, M. Farooq, J. A. Darwish, S. H. Shahbaz, M. Q. Shahbaz, Truncated Weibull-exponential distribution: Methods and applications, *Sci. Rep.,* **13** (2023), 20849. https://doi.org/10.1038/s41598-023-48288-x

3. S. Abid, R. Abdulrazak, [0, 1] truncated Frechet-Weibull and Frechet distributions, *Int. J. Res. Ind. Eng.,* **7** (2018), 106–135. https://doi.org/10.22105/riej.2018.100865.1020
4. A. Ahmad, S. Q. U. Ain, A. Ahmad, R. Tripathi, Bayesian estimation of inverse Ailamujia distribution using different loss functions, *J. Xi'an Univ. Archit. Technol.,* **12** (2020), 226–238.
5. A. Algarni, A. M. Almarashi, F. Jamal, C. Chesneau, M. Elgarhy, Truncated inverse Lomax generated family of distributions with applications to biomedical data, *J. Med. Imag. Health Inform.,* **11** (2021), 2425–2439. https://doi.org/10.1166/jmihi.2021.3733
6. A. M. Almarashi, M. Elgarhy, F. Jamal, C. Chesneau, The exponentiated truncated inverse Weibull-generated family of distributions with applications, *Symmetry,* **12** (2020), 650. https://doi.org/10.3390/sym12040650
7. G. Alomani, M. Kayid, A. M. Elgazar, Classical and Bayesian analysis with fitting radiation data: Using a new truncated distribution, *J. Radiat. Res. Appl. Sci.,* **18** (2025), 101498. https://doi.org/10.1016/j.jrras.2025.101498
8. G. Alomani, M. Kayid, A. M. Elgazar, Statistical analysis of radiation data using power unit moment exponential distribution, *J. Radiat. Res. Appl. Sci.,* **18** (2025), 101432. https://doi.org/10.1016/j.jrras.2025.101432
9. R. A. R. Bantan, C. Chesneau, F. Jamal, I. Elbatal, M. Elgarhy, The truncated Burr XG family of distributions: Properties and applications to actuarial and financial data, *Entropy,* **23** (2021), 1088. https://doi.org/10.3390/e23081088
10. R. A. R. Bantan, F. Jamal, C. Chesneau, M. Elgarhy, Truncated inverted Kumaraswamy generated family of distributions with applications, *Entropy,* **21** (2019), 1089. https://doi.org/10.3390/e21111089
11. J. Burkardt, *The truncated normal distribution*, Department of Scientific Computing Website, Florida State University, **1** (2014), 58. https://doi.org/10.1038/165444a0
12. S. M. Burroughs, S. F. Tebbens, The upper-truncated power law applied to earthquake cumulative frequency-magnitude distributions: Evidence for a time-independent scaling parameter, *Bull. Seismol. Soc. Am.,* **92** (2002), 2983–2993. https://doi.org/10.1785/0120010191
13. R. C. H. Cheng, N. A. K. Amin, Estimating parameters in continuous univariate distributions with a shifted origin, *J. R. Stat. Soc. Ser. B (Methodol.),* **45** (1983), 394–403. https://doi.org/10.1111/j.2517-6161.1983.tb01268.x
14. W. Deng, J. Wang, X. Wu, H. Xi, A novel goodness of fit test for the truncated and non-truncated Yule distributions, *Stat. Pap.,* **66** (2025), 1–18. https://doi.org/10.1007/s00362-025-01721-x
15. A. M. El Gazar, M. ElGarhy, B. S. El-Desouky, Classical and Bayesian estimation for the truncated inverse power Ailamujia distribution with applications, *AIP Adv.,* **13** (2023), 125104. https://doi.org/10.1063/5.0174794
16. A. S. Hassan, M. A. Sabry, A. M. Elsehetry, Truncated power Lomax distribution with application to flood data, *J. Stat. Appl. Probab.,* **9** (2020), 347–359. https://doi.org/10.18576/jsap/090214
17. A. Hassan, M. Sabry, A. Elsehetry, A new probability distribution family arising from truncated power Lomax distribution with application to Weibull model, *Pak. J. Stat. Oper. Res.,* **16** (2020), 661–674. https://doi.org/10.18187/pjsor.v16i4.3442

18. H. S. Jabarah, A. H. Tolba, A. T. Ramadan, A. I. El-Gohary, The truncated unit Chris-Jerry distribution and its applications, *Appl. Math.,* **18** (2024), 1317–1330. https://doi.org/10.18576/amis/180613

19. K. Jayakumar, K. K. Sankaran, Generalized exponential truncated negative binomial distribution, *Amer. J. Math. Manag. Sci.,* **36** (2017), 98–111. https://doi.org/10.1080/01966324.2017.1295892

20. B. A. Kalaf, F. S. M. Batah, A. I. Abdul-Nabi, Right truncated Shankar distribution and its properties, *Ibn AL-Haitham J. Pure Appl. Sci.,* **38** (2025), 493–499. https://doi.org/10.30526/38.1.4031

21. Y. M. Kantar, I. Usta, Analysis of the upper-truncated Weibull distribution for wind speed, *Energ. Convers. Manage.,* **96** (2015), 81–88. https://doi.org/10.1016/j.enconman.2015.02.063

22. T. Kumari, A. Chaturvedi, A. Pathak, Estimation and testing procedures for the reliability functions of Kumaraswamy-G distributions and a characterization based on records, *J. Stat. Theory Pract.,* **13** (2019), 1–41. https://doi.org/10.1007/s42519-018-0014-7

23. J. Mazucheli, A. F. Menezes, S. Dey, Unit-Gompertz distribution with applications, *Statistica,* **79** (2019), 25–43. https://doi.org/10.6092/issn.1973-2201/8497

24. F. Mostafa, M. R. Haque, M. M. Rahman, F. Nasrin, Bayesian inference for left-truncated log-logistic distributions for time-to-event data analysis, *arXiv preprint*, 2025. https://doi.org/10.48550/arXiv.2506.17852

25. O. J. Obulezi, I. C. Anabike, O. G. Oyo, C. Igbokwe, H. Etaga, Marshall-Olkin Chris-Jerry distribution and its applications, *Int. J. Innov. Sci. Res. Technol.,* **8** (2023), 522–533. https://doi.org/10.5281/zenodo.7949632

26. R. C. Patel, Estimates of parameters of truncated inverse Gaussian distribution, *Ann. I. Stat. Math.,* **17** (1965), 29–33. https://doi.org/10.1007/BF02868150

27. E. J. G. Pitman, *Some basic theory for statistical inference (Monographs on Applied Probability and Statistics)*, 1 Ed., Chapman and Hall/CRC, 2018. https://doi.org/10.1201/9781351076777

28. A. T. Ramadan, A. H. Tolba, B. S. El-Desouky, A unit half-logistic geometric distribution and its application in insurance, *Axioms,* **11** (2022), 676. https://doi.org/10.3390/axioms11120676

29. B. Ranneby, The maximum spacing method. An estimation method related to the maximum likelihood method, *Scand. J. Stat.,* **11** (1984), 93–112. Available from: `http://www.jstor.org/stable/4615946`.

30. J. J. Swain, S. Venkatraman, J. R. Wilson, Least-squares estimation of distribution functions in Johnson's translation system, *J. Stat. Comput. Simul.,* **29** (1988), 271–297. https://doi.org/10.1080/00949658808811068

31. A. H. Tolba, Bayesian and non-Bayesian estimation methods for simulating the parameter of the Akshaya distribution, *Comput. J. Math. Stat. Sci.,* **1** (2022), 13–25. https://doi.org/10.21608/cjmss.2022.270897

32. L. Zaninetti, M. Ferraro, On the truncated Pareto distribution with applications, *Open Phys.,* **6** (2008), 1–6. https://doi.org/10.2478/s11534-008-0008-2

33. R. A. ZeinEldin, C. Chesneau, F. Jamal, M. Elgarhy, A. M. Almarashi, S. Al-Marzouki, Generalized truncated Fréchet generated family distributions and their applications, *Comput. Model. Eng. Sci.,* **126** (2021), 791–819. https://doi.org/10.32604/cmes.2021.012169

34. G. C. Canavos, C. P. Tsokos, *A study of an ordinary and empirical Bayes approach to reliability estimation in the gamma life testing model*, Annual Symposium on Reliability, IEEE, 1971.

AIMS Press